Deltares

3D DCSM-FM with water quality: Model set-up and validation

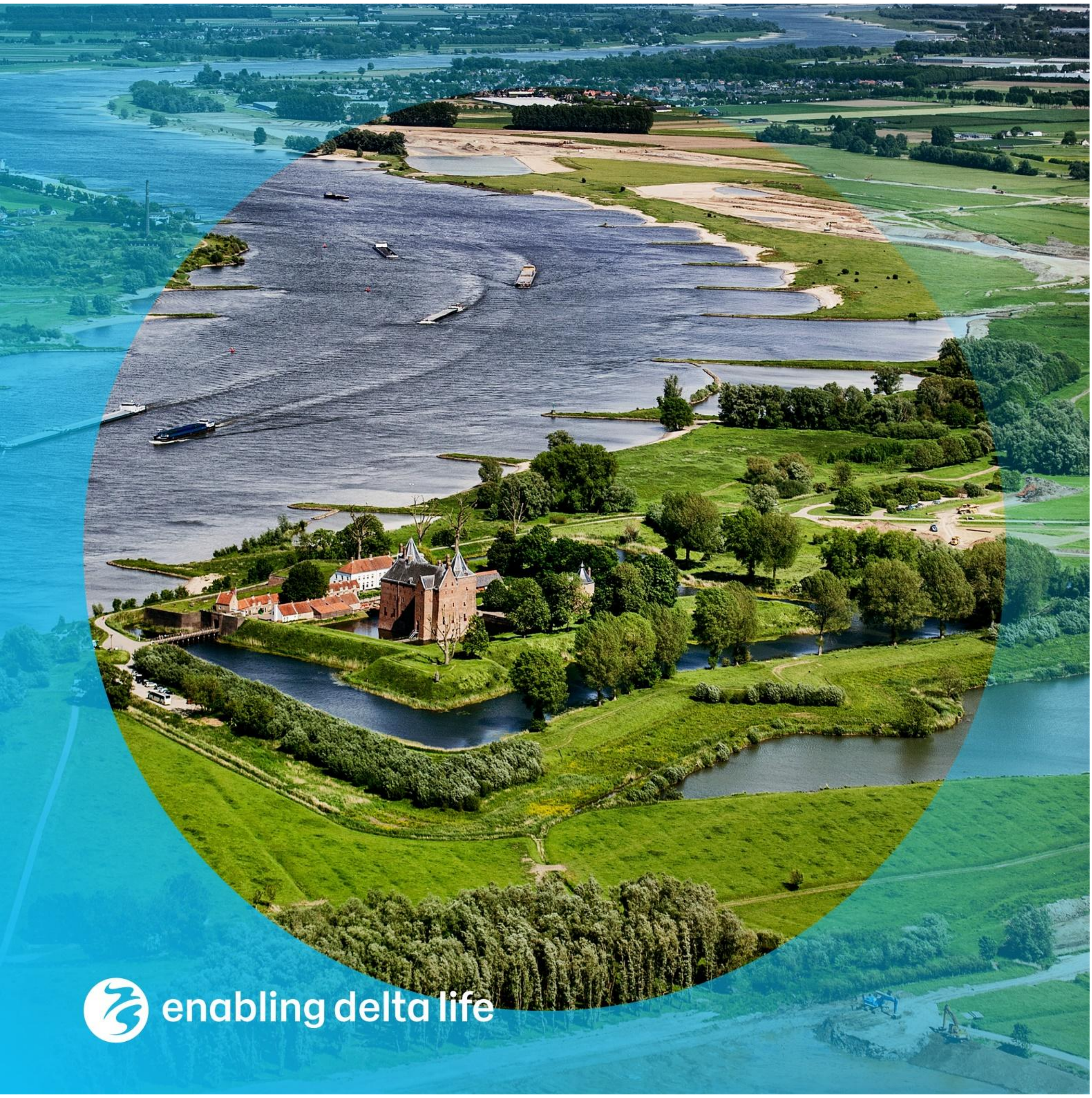

3D DCSM-FM with water quality: Model set-up and validation

Author(s)
Lauriane Vilmin
Sonia Heye
Francesca Di Paola
Anouk Blauw

3D DCSM-FM with water quality: Model set-up and validation

Client	Rijkswaterstaat Water, Verkeer en Leefomgeving
Contact	Muriel Heldring
Projectreference	Referenties
Keywords	North Sea, water quality modelling, nutrients, chlorophyll-a, oxygen, validation

Document control	
Version	1.1
Date	20-02-2026
Project nr.	11211532-003
Document ID	11211532-003-ZKS-0003
Pages	44
Classification	
Status	Final

Author(s)		
	Lauriane Vilmin	
	Sonia Heye	
	Francesca Di Paola	
	Anouk Blauw	

The allowed use of this table is limited to check the correct order-performance by Deltares. Any other client-internal-use and any external distribution is not allowed.

Doc. version	Author	Reviewer	Approver
1.0	Lauriane Vilmin	Tineke Troost	Joost Icke
	Sonia Heye Francesca Di Paola Anouk Blauw		

Summary

The 3D DCSM-FM water quality model has been developed over the past years within various projects to answer a range of questions related to water quality and ecology. This has resulted in several versions of the water quality model, each based on a different hydrodynamic schematization. The goal of this report is to provide a comprehensive overview of the most up-to-date version of the 3D DCSM-FM water quality model. This version has been updated specifically for 2023 OSPAR applications focussing on river nutrient load scenarios (Prins et al., 2023) and has been applied and validated for the years 2015-2017. It is based on the latest hydrodynamics model schematization release (*dflowfm3d-noordzee_0_5nm-j22_6-v1a*) and has the most up-to-date water quality process representation.

This report provides a thorough overview of the model set-up: simulated variables and processes, model forcings and the software used. In addition, the model results and accuracy are assessed for major biogeochemical variables using map plots, time-series and the calculation of model skill metrics, with a focus on monitoring locations from the Dutch national monitoring network (MWTL stations).

The results show that the model performs very well for the simulation of temperature, stratification and winter nutrient concentrations. The model tends to underestimate phosphate in summer, likely pointing to the fact that phosphorus uptake by phytoplankton is too high. Also, the model overestimates nitrate, suggesting that nitrogen re-mineralization rates might be too high. Chlorophyll-a concentrations are overall well represented nearshore but are systematically overestimated during the growing-season in offshore areas. Winter dissolved oxygen seems to be slightly overestimated by the model, but summer minima are all well captured. Based on plotted outputs, we recommend not to use the model for applications in the Baltic Sea, where the model clearly underestimates phosphate and chlorophyll-a concentrations and overestimates dissolved oxygen, probably due to an underestimation of phosphorus at the Baltic inflow boundaries.

This version of the 3D DCSM-FM model is suitable for (and has been applied for) studies investigating effects of river nutrient loads on North Sea eutrophication and large-scale low trophic aquaculture scenarios. As inorganic suspended sediments are not dynamically simulated but included via a forcing function based on remote sensing data, this version of the model is not directly applicable for management questions relating to activities that could affect sediment dynamics (e.g. sand mining, offshore wind developments). The model also doesn’t simulate zooplankton dynamics, which limits its use for applications focussing on the effects on higher trophic levels.

We recommend for future schematization releases to refine the model validation also outside of the Dutch North Sea, for example by calculating and aggregating skill metrics results over different OSPAR assessment areas and investigate new satellite products that could be better adapted to validate different areas of the system (e.g. offshore waters vs turbid areas). We also recommend to validate intermediate variables, such as light extinction, phytoplankton species composition or primary production (if measurements are available), to assess the performance of the model in representing specific underlying processes. Finally, we recommend to include zooplankton in future versions, as this might improve the representation of phytoplankton dynamics in the model and since it is a crucial link to understanding changes in transfers through the marine food chain.

In order to work towards a single model version for the assessment of effects of future marine uses on the North Sea ecosystem, the model version presented here will serve as a basis for future model schematization releases.

Contents

1 Introduction: 3D DCSM-FM with water quality

The 3D DCSM-FM water quality model is a 3D hydrodynamics and biogeochemistry model covering the North Western European Continental Shelf and adjacent waters. The model has been developed at Deltares using the Delft3D Flexible Mesh software suite.

The main purpose of 3D DCSM-FM (standing for Dutch Continental Shelf Model - Flexible Mesh) developments is to have a versatile model that can be used for studies and research on the Northwest European Continental Shelf, including the North Sea and adjacent shallow seas, such as the Wadden Sea. 3D DCSM-FM consists of a hydrodynamic component and a water quality component, each initially developed with their own focus and based on their own history.

The 3D DCSM-FM hydrodynamics schematization releases aim to combine state-of-the-art capabilities with respect to modelling of water levels (tide and surge) as well as (residual) transport phenomena, the latter being crucial for application in water quality and ecological modelling (Zijl, et al., 2023).

The water quality and ecology component has been built on previous model versions for the North Sea, developed over more than 30 years (Los & Blaas, 2010). The 3D DCSM-FM water quality model has been developed over the past years, and within several projects, to answer various questions in terms of water quality and ecology. This has resulted in the development of various versions of the water quality model, each based on a different hydrodynamic schematization. The current 3D DCSM-FM water quality schematization release (*dflowfm3d_dwaq_0_5nm-j17_6_v1*) was developed for applications for the OSPAR Intersessional Correspondence Group on Ecological Modelling (ICG-EMO), focussing on the definition of thresholds for eutrophication (Lenhart et al., 2022; van Leeuwen et al., 2023).

In 2023, the OSPAR model was updated for studies on river nutrient load scenarios (Prins et al., 2023). This version of the model was based on the latest hydrodynamics schematization release (*dflowfm3d-noordzee_0_5nm-j22_6-v1a*). The rest of the model set-up is similar to the *dflowfm3d_dwaq_0_5nm-j17_6_v1* 3D DCSM-FM water quality schematization release, but some improvements have been implemented:

- A dissolved organic fraction has been added to the model's water quality constituents. This results in a slowing down of the recycling of organic matter, leading to lower availability of nutrients in the system. As a consequence, the overestimation of dissolved inorganic nitrogen concentrations at monitoring stations was slightly reduced and the representation of chlorophyll-a concentrations was improved.
- The forcing field for inorganic suspended sediments was improved in the Wadden Sea by using 100 x 100 m Sentinel-2 satellite data instead of MERIS for that area.

The OSPAR 2023 model version has been applied and validated for the years 2015-2017.

In the past years, the need for a single model version for the assessment of effects of future marine uses on the North Sea ecosystem, especially in the context of increasing multi-use, has been pointed out. We intend to develop future model schematization releases based on the version presented here, as it is to this point the most applied and thoroughly validated version (over multiple years).

The goal of this report is to provide a comprehensive overview of this 2023 OSPAR version of the 3D DCSM-FM water quality model . In Chapter 2 the model set-up is described, including the simulated processes, the methods used to derive the different model forcings and the software used. In Chapter 3, the model's performance to represent abiotic and biotic variables relevant for ecosystem functioning is evaluated. The model accuracy is assessed through various methodologies, including maps, time-series and model skill metrics. Finally, chapter 4 provides information on potential applications and limitations of the model.

2 Model set-up

2.1 Computational grid, bathymetry and bottom roughness

3D DCSM-FM covers the Northwest European Continental Shelf, specifically the area between 15°W to 13°E and 43°N to 64°N. The model grid comprises approximately 630,000 unstructured grid cells. The flexible mesh has coarser grid cells near the open boundaries and deep waters, whereas the resolution increases toward the shallower waters. This allows for better matching the spatial scales of the locally relevant physical processes. The grid comprises mostly rectangular grid cells with a number of transition zones between areas of different resolution. Transition zones are created using triangular grid cells.

Cells in deep oceanic waters have a resolution of 1/10° in the longitudinal direction and 1/15° in the latitudinal direction, corresponding to approximately 4 by 4 nautical miles (nm) over the entire domain. Along all coasts and in the southern North Sea, cell sizes decrease to 0.5 by 0.5 nm, corresponding to approximately 900 m (Figure 2-1).

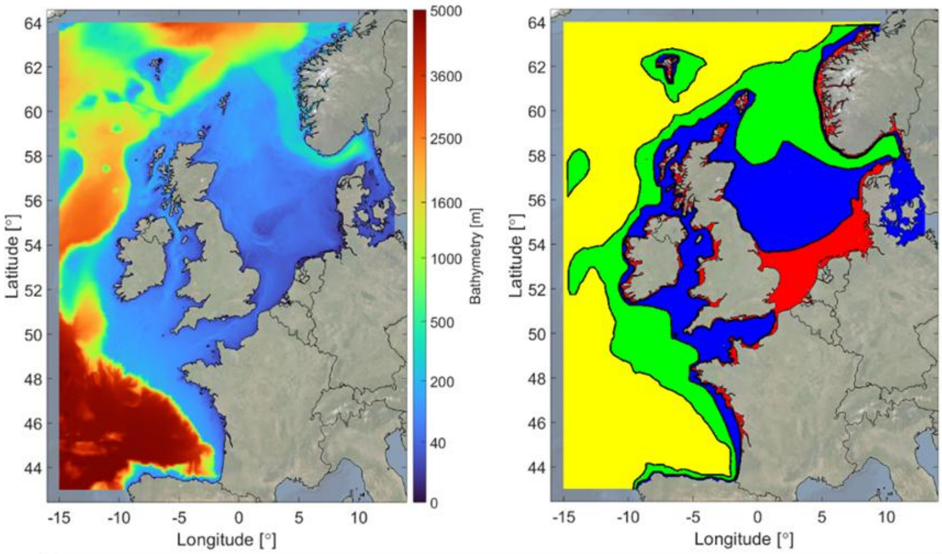

Yellow:	1/10° x 1/15°	~ 4.0 nm x 4.0 nm	
Green:	1/20° x 1/30°	~ 2.0 nm x 2.0 nm	→800m isobath
Blue:	1/40° x 1/60°	~ 1.0 nm x 1.0 nm	→200m isobath
Red:	0.75' x 0.5'	~ 0.5 nm x 0.5 nm	→ 50m isobath

Figure 2-1: Domain, bathymetry and grid cell size of 3D DCSM-FM.

A z-sigma-layer approach is used for the vertical schematization of the model. Down to a depth of 100 m, the water column is divided into 20 layers of equal thickness (sigma-layers). In deeper areas, the water column is further divided into a maximum of 30 layers at fixed depths (z-layers), gradually increasing in thickness, each subsequent layer being 19% thicker.

The model bathymetry is based on the gridded dataset by the European Marine Observation and Data Network (EMODnet) from December 2020. For large parts of the Dutch waters, bathymetric information from the detailed baseline database by the Dutch government is used.

For the bed friction, a spatially varying Manning roughness coefficient is used. The bottom roughness field was calibrated using OpenDA-DUD to obtain an optimal water level representation (Zijl, et al., 2023).

2.2 Simulated variables and processes

2.2.1 Hydrodynamics

D-Flow FM computes water levels (tide and surge), currents as well as temperature and salinity (Deltares, 2023a). For more details on the methods and parameterization of the hydrodynamic component of the model, refer to Zijl et al. (2021, 2023).

2.2.2 Water quality

Biogeochemical processes are simulated using the D-Water Quality module. Process representations are selected from the D-Water Quality Process Library (Deltares, 2023). The main features and parameterization of the water quality component are initially derived from the Generic Ecological Model for estuaries and coastal waters by Blauw et al. (2009), adapted to the newer D-Flow FM software and further developed in a range of studies (Lenhart et al., 2022; Prins et al., 2023; Zijl, et al., 2021; Zijl, et al., 2023).

The water quality component of the model simulates the cycles of major nutrients (nitrogen, phosphorus and silica), organic carbon and dissolved oxygen. The model's water quality state variables are listed and described in Table 2-1.

Simulated processes are represented in Figure 2-2. These include:

- Phytoplankton photosynthesis (affected by the underwater light climate, which in turn is affected by light extinction), associated uptake of nutrients and carbon dioxide and production of oxygen;
- Light extinction by inorganic suspended matter, organic matter and phytoplankton;
- Phytoplankton respiration and mortality, and the associated release of nutrients (partly detritus, partly inorganic) and dead organic carbon and consumption of oxygen;
- Settling of dead organic matter and phytoplankton (and eventually burial in the sediment);
- Remineralization of organic matter (detritus) in the water column and in the sediment, both leading to oxygen consumption;
- Dissolution of biogenic silica in the water column and in the sediment;
- Nitrification and the associated consumption of oxygen;
- Denitrification in the water column and in the sediment;
- Atmospheric deposition of ammonium and nitrate;
- Oxygen re-aeration at the water surface.
- Grazing by bottom filter-feeders (*Mytilus edulis* and *Ensis*) on phytoplankton and detritus in the water column.

Phytoplankton dynamics (primary production, respiration and mortality) are simulated using the BLOOM module (Los & Blaas, 2010; Los & Brinkman, 1988, Blauw et al., 2009). BLOOM simulates growth, competition and adaptation of phytoplankton to nutrient or light-limiting conditions at daily intervals. Here, four functional groups are simulated: marine diatoms, flagellates, dinoflagellates and *Phaeocystis*.

For each of these groups, three ecotypes are defined to account for adaptation to specific environmental conditions:

- an energy type ("_E"), adapted to low light conditions, with relatively high growth rate, low mortality rate and high N:C and P:C ratio, and higher chlorophyll-a content;
- a nitrogen type ("_N"), adapted to low N concentrations, with typically lower internal N:C ratio, lower maximum growth rate, higher mortality rate, higher settling velocity and lower chlorophyll-a content;
- a phosphorus type ("_P"), adapted to low P concentrations, similar to the nitrogen type with typically lower internal P:C ratio.

BLOOM assumes that fast-growing phytoplankton (energy type) dominate in situations where light and nutrient resources are abundant, while slow-growing, nutrient-efficient phytoplankton species become dominant when resources become limited (Blauw et al., 2009). When conditions in the water change, one phenotype can be instantaneously converted into another phenotype of the same functional group. This represents the rapid adaptation of individual algal cells. Species composition is calculated using linear programming to maximize the total net production of the whole phytoplankton community, depending on the prevailing conditions.

Grazer dynamics are simulated with the DEBGRZ module (Troost et al., 2010). DEBGRZ is based on the Dynamic Energy Budget (DEB) theory (Kooijman, 2009), with adaptations to the equations that translate the life cycle of individuals to the dynamics of entire grazer populations and their feedback on the ambient environment. This is used to simulate the dynamics and effects of *Mytilus edulis* (blue mussel) populations in the Wadden Sea and *Ensis* (razor clams) in the rest of the model domain.

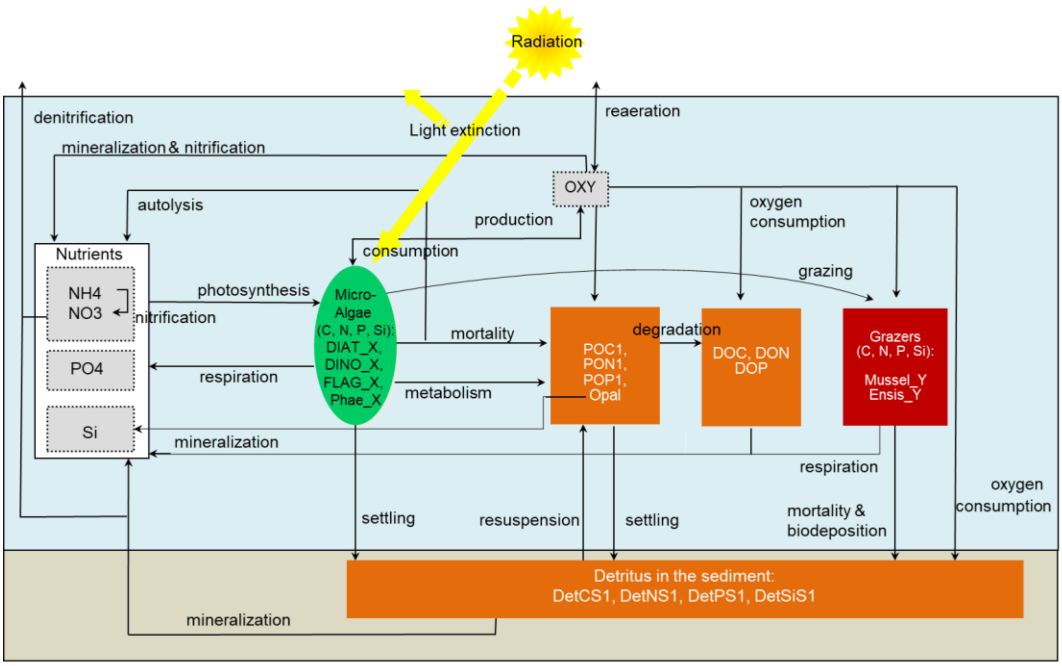

Figure 2-2: Scheme of variables and processes simulated with D-Water Quality in the 3D DCSM-FM water quality model. X ∊ [E, N, P], Y ∊ [V, E, R]. For definition of the model's state variables, see Table 2 1.

Table 2-1: Description of model state variables. Conversion factors from CMEMS variables used for offshore boundaries and initial state.

D-Water Quality state variable [unit]	Description	Active*	CMEMS variable [unit]	Conversion factor	Source
OXY [g/m3]	Dissolved oxygen	x	o2 [mmol/m3]	32/1000	
NH4 [gN/m3]	Ammonium	x	-	-	
NO3 [gN/m3]	Nitrate	x	no3 [mmol/m3]	14/1000	
PO4 [gP/m3]	Phosphate	x	po4 [mmol/m3]	30.97/1000	
Si [gSi/m3]	Silica	x	si [mmol/m3]	28.08/1000	
POC1 [gC/m3]	Detrital Particulate Organic Carbon	x	phyc [mmol/m3]	2*(12/1000)	[1]
PON1 [gN/m3]	Detrital Particulate Organic Nitrogen	x	phyc [mmol/m3]	2*(16/106)*(14/1000)	[1-2]
POP1 [gP/m3]	Detrital Particulate Organic Phosphorus	x	phyc [mmol/m3]	2*(1/106)*(30.97/1000)	[1-2]
Opal [gSi/m3]	Biogenic silica	x	phyc [mmol/m3]	0.5*0.13*(28.08/1000)	[3]
DOC [gC/m3]	Dissolved Organic Carbon	x	phyc [mmol/m3]	(91.8/8.2)*2*(12/1000)	[1,4]
DON [gN/m3]	Dissolved Organic Nitrogen	x	phyc [mmol/m3]	(19/225)*(91.8/8.2)*2*(14/1000)	[1,4-5]
DOP [gP/m3]	Dissolved Organic Phosphorus	x	phyc [mmol/m3]	(1/225)*(91.8/8.2)*2*(30.97/1000)	[1,4-5]
DIAT_X, DINO_X, FLAG_X, Phae_X (X ∊ [E, N, P]) [gC/m3]	Diatoms, dinoflagellates, flagellates and Phaeocystis (energy-, nitrogen- and phosphorus-limited)	x	-	-	
DetCS1 [gC/m2]	Detrital Carbon in the sediment		-	-	
DetNS1 [gN/m2]	Detrital Nitrogen in the sediment		-	-	
DetPS1 [gP/m2]	Detrital Phosphorus in the sediment		-	-	
DetSiS1 [gSi/m2]	Detrital Silica in the sediment		-	-	
Mussel_V, Mussel_E, Mussel_R [gC/m2]	Mussel structural biomass, energy reserves and gonadal biomass		-	-	
Ensis_V, Ensis_E, Ensis_R [gC/m2]	Ensis structural biomass, energy reserves and gonadal biomass		-	-	

* “Active substances” are those that can be transported by advection/diffusion processes

[1] Assuming a carbon detritus to algae ratio of 2
[2] Using the molar Redfield C:N:P ratio 106:16:1 (Redfield, 1934)
[3] Using the C:Si ratio for diatoms from Brzezinski (1985) and assuming that half of the phytoplankton carbon biomass is constituted by diatoms
[5] Assuming 91.8% of offshore organic matter is dissolved (estimate for waters of the shelf currents from (Agatova et al., 2008))
[6] Using a molar C:N:P ratio of 225:19:1 (global average export stoichiometry of semi-labile dissolved organic matter below 100m estimated by (Letscher et al., 2015))

2.3 Model forcings

2.3.1 Meteorological forcings

3D DCSM-FM uses atmospheric boundary conditions from ECMWF's ERA5 reanalysis dataset (https://cds.climate.copernicus.eu/datasets/reanalysis-era5-single-levels?tab=overview). This includes hourly 2D fields for 10 m eastward and northward wind components, Charnock coefficient, 2 m air and dewpoint temperatures, cloudiness, long wave and short wave solar radiations, maximum evaporation and total precipitation rates. For more details, refer to Zijl et al. (2021, 2023).

2.3.2 Open boundaries

2.3.2.1 Water levels

Water level boundaries are applied at the northern, western and southern open boundaries. Here, astronomical water levels are imposed, derived from a harmonic expansion of the amplitudes and phase lags of 39 tidal constituents. These constituents are retrieved from the global tide model FES2014. The surge at the open boundaries is approximated by addition of an inverse barometer correction to the astronomical water levels. This correction is a time- and space-dependent function of the local atmospheric pressure. To account for steric effects, the daily mean water levels from CMEMS are used (Global Ocean Physics Reanalysis product, https://data.marine.copernicus.eu/product/GLOBAL_MULTIYEAR_PHY_001_030/description)

2.3.2.2 Salinity, temperature and water velocities

As for water levels, salinity, water temperature and seawater velocities (eastward and northward components) at the northern, western and southern open boundaries are forced using daily data from the CMEMS Global Ocean Physics Reanalysis product. These daily values at 50 non-uniformly spaced vertical levels are interpolated by D-Flow FM to the right horizontal location and model layers.

2.3.2.3 Water quality variables

Concentrations of water quality state variables are forced at the northern, western and southern open boundaries using monthly data from the CMEMS Global Ocean Biogeochemistry Hindcast product (https://data.marine.copernicus.eu/product/GLOBAL_MULTIYEAR_BGC_001_029/description). These monthly values at 75 non-uniformly spaced vertical levels are interpolated by D-Flow FM to the right horizontal location and model layers. The conversion factors used to derive concentrations of the simulated D-Water Quality state variables from available CMEMS variables are provided in Table 2-1.

2.3.3 Baltic boundary

The Baltic boundary is represented by two point sources entering the model domain within the Dars (54.459°N, 12.084°E) and Drogden (55.344°N, 12.707°E) straits. At these shallow sills the predominant flow direction is from the Baltic Sea to the Kattegat. A climatology of mean monthly discharges was calculated based on monthly data provided by DHI for 2002-2019. Nutrient concentrations were derived from monitoring data provided by Stiig Markager (Arhus University, DK). For silicate, an estimate of 10.4 µM was used, based on data in a paper by Bentzon-Tilia et al. (2015). Detailed methods to derive the concentrations of water quality variables are described in (Lenhart et al., 2022; Prins et al., 2021).

2.3.4 Freshwater discharges

Freshwater discharges are defined using the ICG-EMO river database, maintained by Sonja van Leeuwen (NIOZ, https://doi.org/10.25850/nioz/7b.b.vc). Methods to translate the data to model inputs are described in (Lenhart et al., 2022). This data is based on available observations and model estimates provided by the OSPAR member states that are interpolated to daily values. The availability of observations differs per country. For example, some countries measure both nitrate, ammonium and total nitrogen concentrations, whereas other countries only measure nitrate and ammonium in their rivers. Organic nutrient concentrations have been estimated as total nutrient concentrations (N or P) minus dissolved inorganic nutrient concentrations (N or P). For the rivers where observations of total nutrient concentrations were lacking, we estimated the organic nutrient loads from winter inorganic nutrient concentrations. To this end, we calculated a climatology of the ratio between organic nutrient concentrations (as function of day of the year) and winter mean dissolved inorganic nutrient concentrations for all the rivers where total nutrient concentrations were available. The mean of this ratio over all rivers in the database (separate for N and P) was used to calculate the organic nutrient concentrations for rivers where total nutrient observations was lacking. If no total or particulate organic carbon data was available, organic carbon was derived from organic nitrogen using the C:N weight ratio of 12, estimated for global riverine total organic material by Meybeck (1982) The concentrations of dissolved and particulate fractions of organic carbon and nutrients were then derived using the ratios of nutrient export estimates for European rivers from (Seitzinger et al., 2005) (DOC:POC1=8:7, DON:PON1=0.7:1.1, DOP:POP1=0.04:0.33).

River temperatures are not provided in the ICG-EMO database. These were forced per country using a monthly climatology of the country's largest river (in terms of discharge), based on EHYPE model outputs for the period 1989-2013.

2.3.5 Atmospheric deposition

Atmospheric deposition is included in the model as an additional source of dissolved nitrogen. The deposition rate is forced using the 2017 total (wet + dry) deposition fields of reduced nitrogen for NH4 and oxidized nitrogen for NO3 from the Norwegian Meteorological Institute (MET Norway). These fields have a 0.1-degree horizontal resolution and were calculated using the EMEP MSC-W chemical transport model (https://emep.int/mscw/mscw_moddata.html).

2.3.6 Inorganic sediments

Inorganic suspended sediments forcing is based on average yearly measurements from satellite data. The satellite data consist of a combination of Sentinel-2 data in the Wadden Sea (https://dataspace.copernicus.eu/data-collections/copernicus-sentinel-data/sentinel-2) and MERIS data (Nechad et al., 2010) over the rest of the domain. A sinusoidal function is applied to the yearly-average 2D field to derive weekly fields (Prins et al., 2023).

The amount of inorganic matter in the bottom sediment is forced using a 2D field derived from model results of a spun-up North Sea fine sediment run carried out for the WOZEP research programme, reported in Zijl, et al. (2023). The field used here does not vary over time. It is used in the calculation of burial rates of detrital organic matter in the sediment.

2.3.7 Initial conditions

The spatially varying salinity and temperature in the model are initialized using 3D spatial fields from the CMEMS Global Ocean Physics Reanalysis product (for 1st January 2012). The concentrations of active water quality state variables were initialized based on 3D fields from the Global Ocean Biogeochemistry Hindcast product, using the same conversion factors as for the model's open boundary forcings (Table 2-1).

NO3 and PO4 initial concentration fields were overwritten on the shelf by linearly interpolated, winter-mean (December-February) in-situ measurements from the EMODnet database for the period 2006-2020. This was done, to limit the model's spin-up time, since the biogeochemistry CMEMS product underestimates nutrient concentrations in the inner North Sea.

Outside of the North Sea, organic detritus in the sediment (DetCS1, DetNS1, DetPS1 and DetSiS1) are forced based on depth-averaged POC1, PON1, POP1 and Opal concentrations that were derived from the CMEMS biogeochemistry product. These were calculated assuming that the settling of the suspended organic matter to the bottom is in equilibrium with the mineralization flux of bottom organic detritus.

Within the North Sea (over the Zuno-DD model domain), initial values for organic detritus in the sediment and for mussel and Ensis variables are forced using model outputs from the Zuno-DD model (van der Kaaij et al., 2017).

2.4 Simulated years

The years 2012-2014 were simulated as spin-up years, to allow the model to reach initial conditions consistent with model inputs. The model was then run and analysed for the years 2015-2017. Water quality processes were calculated at a 10 min time step. Time-series outputs were saved at observation locations at a daily time-step (at midnight) and 3D map outputs were produced at a 5-day time step.

2.5 Software and computational performance

The model was computed using the D-Flow FM module from the 2023.02 software release of the Delft3D Flexible Mesh Suite. Water quality processes are simulated using the D-Water Quality module, which is fully integrated and runs in parallel with D-Flow FM. This integration ensures consistency between the simulated transport of water quality constituents, and the transport of water masses, salt and temperature.

Computations were performed on the Dutch national supercomputer Snellius from SURF. It takes about 2 days and 15h to compute one calendar year using 64 cores on 4 nodes (total of 256) using Snellius's genoa partition (thin nodes).

3 Model validation

3.1 Methodology

3.1.1 Validated variables

In this report we validate model output variables that are relevant for the simulation of the North Sea's ecosystem functioning and for which in-situ measurements are available. These include:

- Water temperature
- Nitrate
- Phosphate
- Chlorophyll-a
- Dissolved oxygen

3.1.2 Maps

Simulated spatial patterns are validated with observed data using maps. These represent multi-year (2015-2017) averages for specific seasons, relevant for the investigated variables. In these maps, we don't show the entire model domain, but zoom into the North Sea (latitudes: 48°N to 62°N, longitudes: 15°W to 13°E). Multi-year aggregations of in-situ observations are represented by coloured dots. These observations are extracted from the North and Wadden Sea Data Management (NWDM) database (https://github.com/Deltares-research/nwdm). This database is maintained by Deltares and includes various data sources from the main data owners of North Sea and Wadden Sea data. It covers 31 parameters and multiple data sources consisting of national databases and data platforms (EMODnet, ICES, SOCAT), covering the period 1893-2024. The data originates from several types of monitoring techniques, such in-situ sampling campaigns, but also observation buoys and ferry boxes.

For near-surface maps, data points from 2015-2017 in the top 5.5 m were extracted. Only locations with at least 6 observations per year are shown for maps representing growing-season means (March–September); locations with at least 3 observations per year are shown for maps of winter (December–February) or summer (June–August) means. In this way, we balanced the need for as many observation locations and the need for statistically representative data for calculating season means. To minimise bias in the observation due to different sampling frequencies per month, first the monthly mean was calculated per variable and then the seasonal mean was based on the monthly means.

Additionally, surface chlorophyll-a concentrations are validated against satellite data from the Copernicus Marine Service Ocean Colour Thematic Assembly Centre (OC TAC). This data source is very useful to validate spatial patterns over the model's extent. It is however known to have larger errors near the coast. The spatial comparison with the satellite data was carried out 1) by plotting the differences in simulated and satellite-derived growing-season mean chlorophyll-a concentrations and 2) by plotting the correlation coefficients between simulated and satellite monthly-average near-surface chlorophyll-a concentrations over 2015-2017 growing seasons and aggregated per OSPAR assessment area (see Figure 3-1 for locations of the assessment areas).

In the map plots, the following seasonal aggregations are made:

- Growing season mean (March to September) for temperature and chlorophyll-a,
- Winter mean (December to February) for nitrate and phosphate,
- Summer mean (June to August) for dissolved oxygen.

3.1.3 Model skill metrics

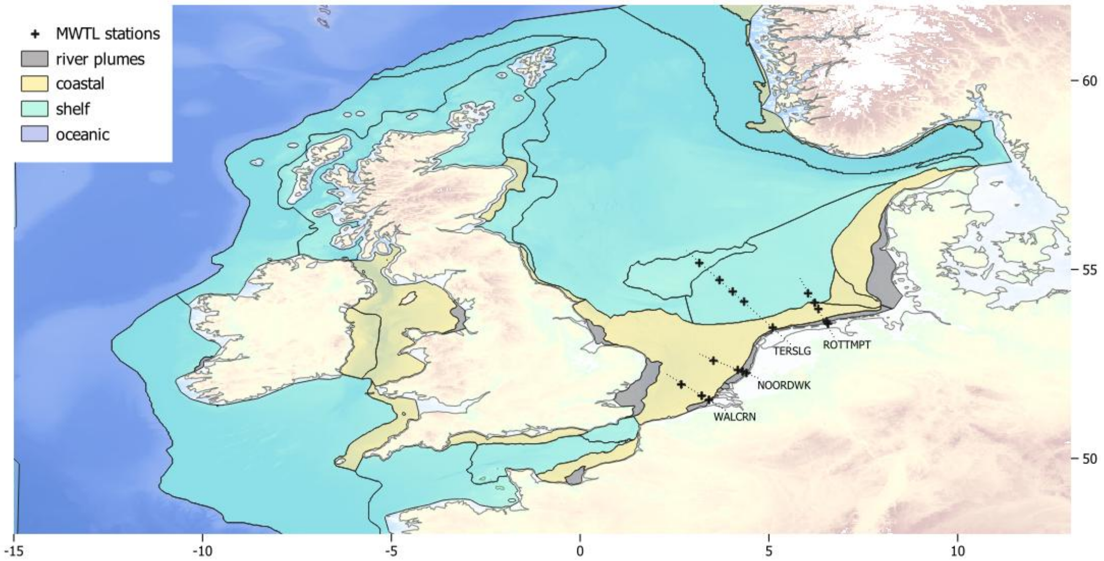

Figure 3-1: Locations of the stations of the Dutch national monitoring program (MWTL stations) used for validation in this report. ROTTMPT=Rottumerplaat transect, TERSLG=Terschelling transect, NOORDWK=Noordwijk transect, WALCRN=Walcheren transect. Colored polygons correspond to OSPAR assessment areas, divided in 4 categories: river plumes, coastal, shelf and oceanic.

For each station of the Dutch national monitoring program (MWTL station) along the Walcheren, Noordwijk, Terschelling, and Rottumerplaat transects (Figure 3 1), the mean and standard deviation of near-surface in-situ observations and model results are calculated and compared for each month from 2015 to 2017. Monthly averages are computed by grouping all available data for each station-variable combination by month (e.g., all January data from 2015, 2016, and 2017 are averaged together), resulting in up to 12 monthly data points per station and variable over the three-year period. The pearson correlation (R) between monthly model results and observations, as well as the Root Mean Square Error (RMSE), and normalized RMSE (RMSE divided by the standard deviation of observations, noted nRMSE) are then calculated and presented in table format (Table 3-2 to Table 3-6). The column 'Number of months' indicates the total number of monthly averages available per station-variable combination over 2015–2017, with a maximum of 12 observations per station. The model skill assessment is summarized in diagrams showing (1 – correlation coefficient) against the nRMSE of monthly-average near-surface values at the MWTL stations over, again over 2015–2017. Correlation coefficients and RMSE values are calculated only for these monthly-averaged values, not for the raw timeseries data. In this way, we reduce the impact of noise and limited statistical representation in monthly observations and focus on the validation of characteristic seasonal patterns per location.

To evaluate model performance against observational data at the MWTL stations, we classify the correlation coefficient (R) and normalized RMSE (nRMSE) into four categories, ranging from very good to limited performance. As we did not identify commonly accepted classification criteria in the literature for coastal biogeochemical models, we therefore propose the classification shown in Table 3-1 to enable a consistent and objective interpretation of our results. The same classification scheme is applied to all variables. It is, however, important to note that some variables are inherently more difficult to predict than others. For example, large-scale ocean models generally simulate salinity and temperature more accurately than nutrient concentrations and typically exhibit lower correlation with observations when simulating primary production (Lovato et al., 2024).

Table 3-1: Evaluation criteria used to qualify the 3D DCSM-FM water quality model performance.

	Limited	Satisfactory	Good	Very good
R	<0.5	0.5-0.6	0.6-0.7	>0.7
nRMSE	>2	1-2	<1	<0.5

3.1.4 Time-series

Time-series of model results and in-situ measurements are plotted at eight stations along the Noordwijk and Terschelling transects from the Dutch national monitoring programme (MWTL stations, see Figure 3-1), for near-surface and near-bottom values. This provides insight in the model's ability to reproduce seasonal variations in validated variables, stratification patterns and differences between near-shore and offshore locations. For chlorophyll-a, time series extracted from the OC TAC satellite data are plotted as well.

3.2 Validation of water temperature

The 3D DCSM-FM model captures the spatial patterns of near-surface water temperatures, with warmer waters along the coasts of the southern North sea and southern Celtic sea and colder waters offshore (Figure 3-2 and Figure 3-3). The spatial gradients observed from in-situ measurements and along ferry box transects are overall well represented. Coldest near-surface temperatures are simulated in the Norwegian Trench and north from the UK (Figure 3-2).

As shown in Table 3-2 and Figure 3-4, the model reproduces very well monthly-average observed near-surface temperatures for 2015-2017, both in terms of values and variability at all MWTL stations, with correlations between observations and model >0.98 and RMSE values mostly below 1°C. The model seems to perform best in terms of RMSE at stations further than 10 km from the coast.

Additionally, the model effectively captures seasonal variations in sea temperatures throughout the year, as evidenced by the time series (Figure 3-5). The model also reproduces near-bottom temperatures well at stations where observations are available. For example, it captures the intensity of temperature stratification at stations TERSLG100 and TERSLG175 in spring and summer.

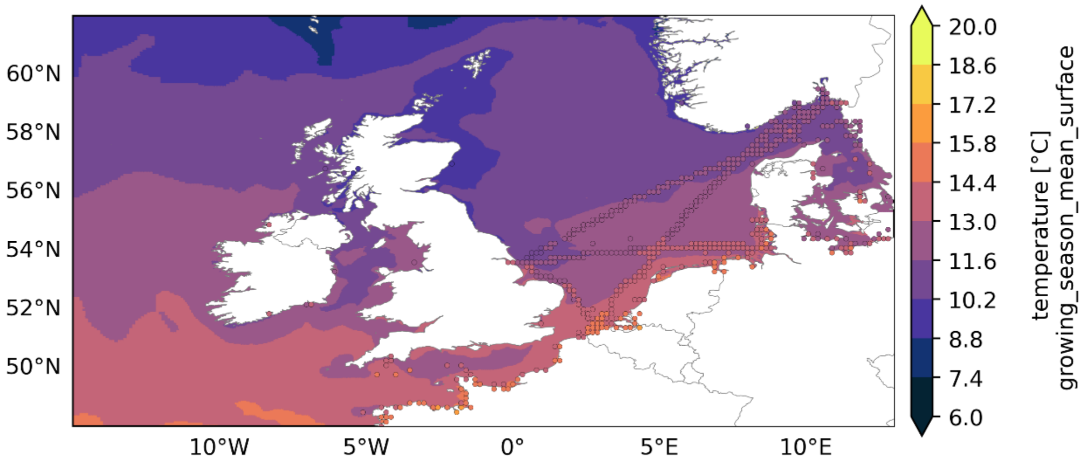

Figure 3-2: Simulated (background) and observed (dots) growing season mean near-surface water temperature for 2015-2017.

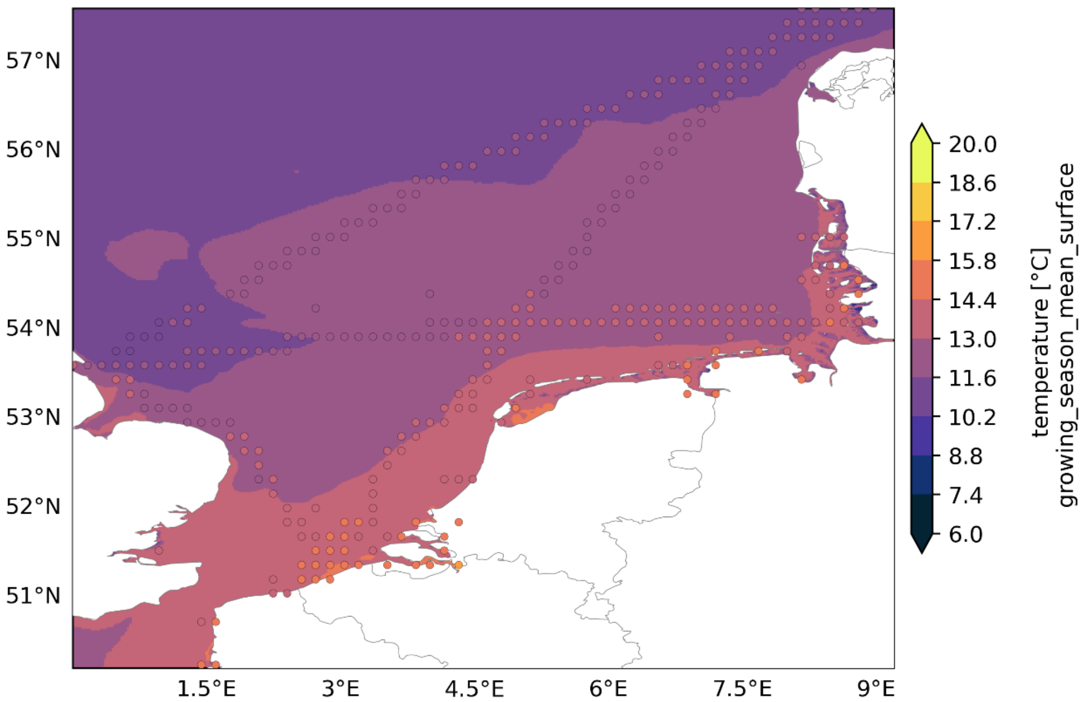

Figure 3-3: : Simulated (background) and observed (dots) growing season mean near-surface water temperature for 2015-2017, zoomed into the Southern North Sea.

Table 3-2: Skill metrics for monthly-average near-surface temperature at MWTL stations over 2015-2017. Colours refer to the evaluation criteria categories from Table 3-1.

Station	Number of months	Mean Obs	Mean DCSM	Std Dev Obs	Std Dev DCSM	Correlation	RMSE	nRMSE
WALCRN2	11	12.69	12.42	5.29	4.99	0.98	1.055	0.20
WALCRN20	12	12.25	12.24	4.74	4.65	0.99	0.742	0.16
WALCRN70	11	12.7	12.65	3.66	3.79	0.99	0.566	0.15
NOORDWK2	12	12.28	11.98	5.23	4.89	0.99	0.981	0.19
NOORDWK10	12	12.29	12.06	5.16	4.81	0.99	0.849	0.16

Station	Number of months	Mean Obs	Mean DCSM	Std Dev Obs	Std Dev DCSM	Correlation	RMSE	nRMSE
NOORDWK20	12	12.07	12.07	4.72	4.71	1.0	0.435	0.09
NOORDWK70	12	12.19	12.02	4.08	4.1	0.99	0.475	0.12
TERSLG10	12	11.98	11.74	4.98	4.67	0.98	0.951	0.19
TERSLG100	6	11.78	11.74	4.04	4.32	1.0	0.366	0.09
TERSLG135	12	11.28	11.21	3.86	4.07	0.99	0.486	0.13
TERSLG175	4	11.04	11.06	4.03	4.15	0.99	0.651	0.16
TERSLG235	4	10.91	10.96	3.81	3.89	0.99	0.399	0.10
ROTTMPT3	12	11.61	11.09	5.21	5.38	0.99	0.921	0.18
ROTTMPT50	4	14.65	14.85	3.15	3.1	0.99	0.408	0.13
ROTTMPT70	4	14.41	14.59	3.22	3.14	0.99	0.424	0.13

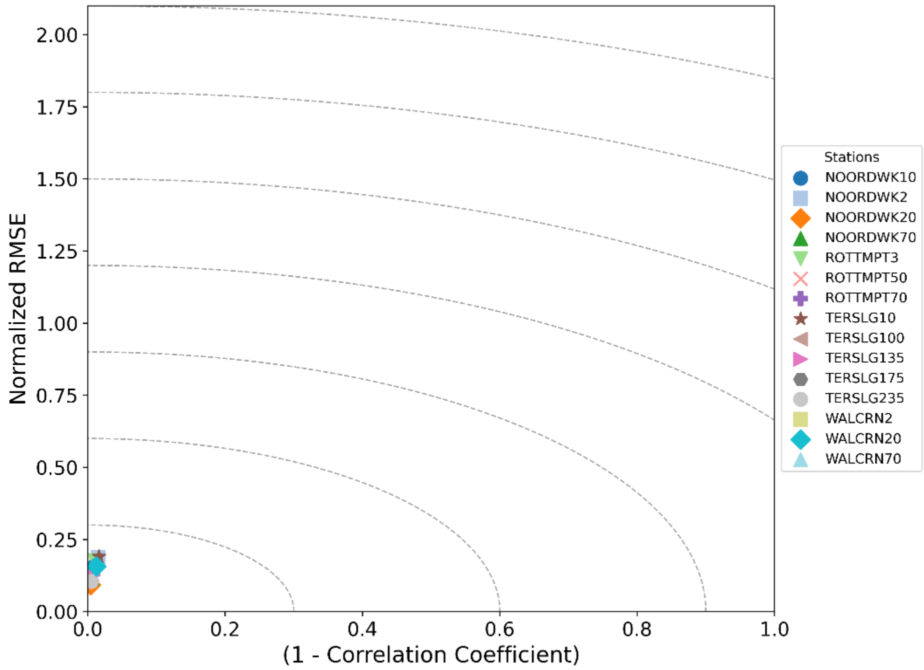

Figure 3-4: Model skill assessment for monthly-average near-surface temperature at the MWTL stations over 2015-2017.

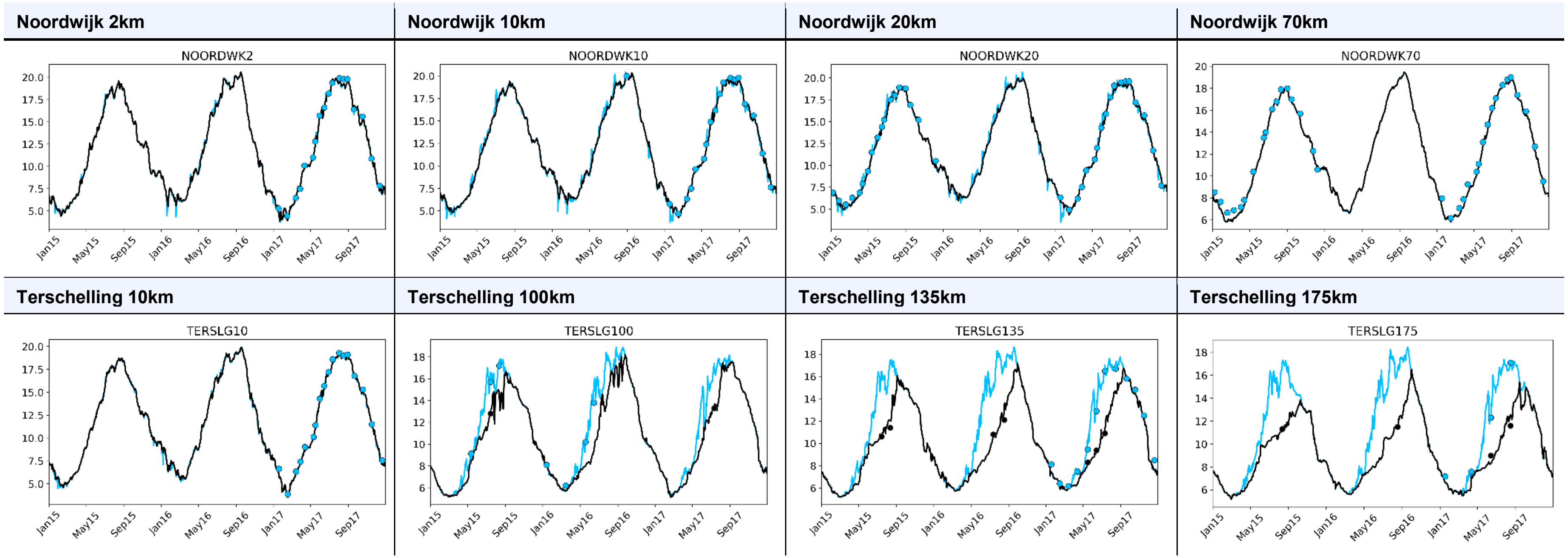

Figure 3-5: Comparison of simulated (lines) and observed (dots) water temperature (in °C) near the surface (blue) and near the bottom (black) along the Noordwijk and Terschelling MWTL transects. Note that the y-axes vary per figure.

3.3 Validation of water quality variables

3.3.1 Nitrate

3D DCSM-FM captures the horizontal spatial patterns of winter mean near-surface nitrate, with high concentrations observed in coastal areas from France, Belgium, the Netherlands, Germany, western Denmark and southern UK, and lower concentrations further offshore and in the Baltic (Figure 3-6 and Figure 3-7).

As shown in Table 3-3 and Figure 3-8, the model reproduces monthly-average near-surface nitrate concentrations well to very well at most MWTL stations, both in terms of correlations and nRMSE. The correlation between observations and model are generally high (values >0.8 in station closer to the coasts and lower offshore) and RMSE mostly below 0.1 gN/m3.

Additionally, the model effectively captures seasonal variations throughout the year, as shown by the time series (Figure 3-9).The model corresponds well with observations in winter, spring and summer. Only in autumn nitrate concentrations increase to winter values faster than in the observations, particularly offshore, explaining the lower correlation between monthly-average observations and model outputs at offshore stations. Offshore, both simulated and observed nitrate concentrations are at the detection limit in summer, suggesting primary production is nitrogen limited in summer, which is in line with literature.

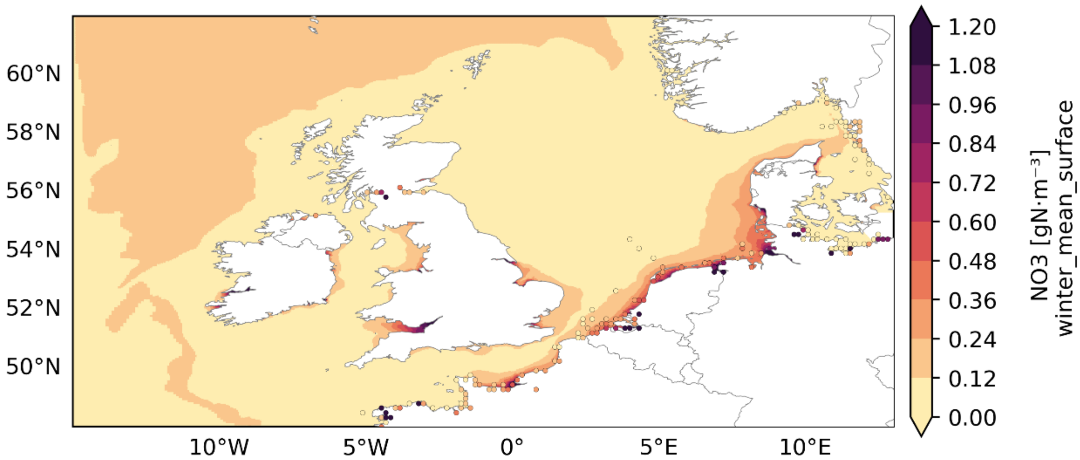

Figure 3-6: Simulated (background) and observed (dots) nitrate winter mean concentration near-surface for 2015-2017.

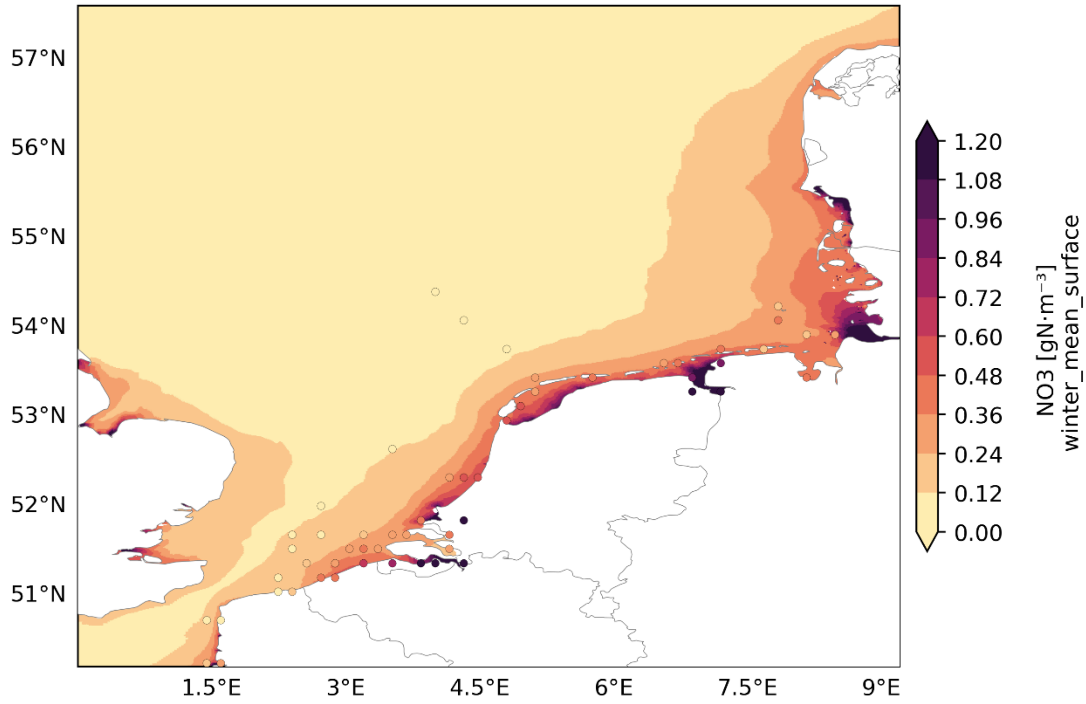

Figure 3-7: Simulated (background) and observed (dots) nitrate winter mean concentration near-surface for 2015-2017, zoomed into the Southern North Sea.

Table 3-3: Skill metrics for monthly-average near-surface nitrate concentrations at MWTL stations for 2015-2017. Colours refer to the evaluation criteria categories from Table 3-1.

Station	Number of months	Mean Obs	Mean DCSM	Std Dev Obs	Std Dev DCSM	Correlation	RMSE	nRMSE
WALCRN2	12	0.17	0.19	0.15	0.11	0.89	0.08	0.53
WALCRN20	12	0.1	0.17	0.1	0.08	0.8	0.09	0.90
WALCRN70	12	0.03	0.07	0.03	0.05	0.74	0.05	1.67
NOORDWK2	12	0.35	0.32	0.22	0.16	0.89	0.11	0.50
NOORDWK10	12	0.26	0.27	0.2	0.13	0.9	0.1	0.50
NOORDWK20	12	0.15	0.21	0.14	0.1	0.8	0.1	0.71
NOORDWK70	12	0.03	0.06	0.03	0.05	0.54	0.06	2.00
TERSLG10	12	0.08	0.14	0.09	0.08	0.78	0.08	0.89
TERSLG100	12	0.03	0.03	0.03	0.03	0.54	0.03	1.00
TERSLG135	12	0.05	0.03	0.08	0.03	0.59	0.07	0.88
TERSLG175	4	0.02	0.02	0.02	0.03	1.0	0.02	1.00
TERSLG235	4	0.03	0.02	0.03	0.03	1.0	0.01	0.33
ROTTMPT3	12	0.15	0.23	0.17	0.15	0.89	0.11	0.65
ROTTMPT50	4	0.01	0.04	0.0	0.01	0.06	0.03	-
ROTTMPT70	4	0.01	0.02	0.0	0.01	-0.35	0.02	-

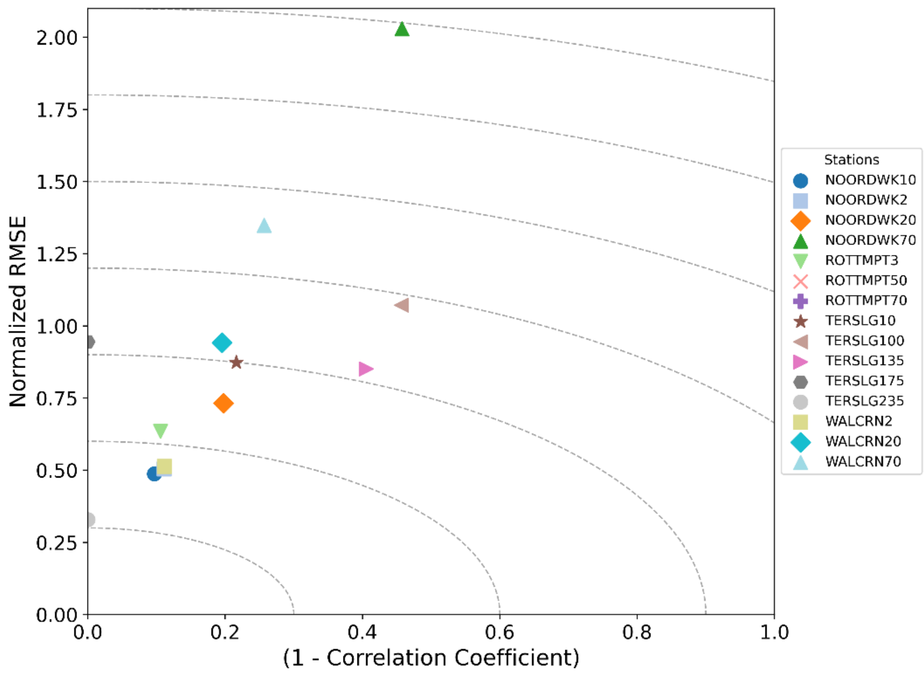

Figure 3-8: Model skill assessment for monthly-average near-surface nitrate at the MWTL stations over 2015-2017.

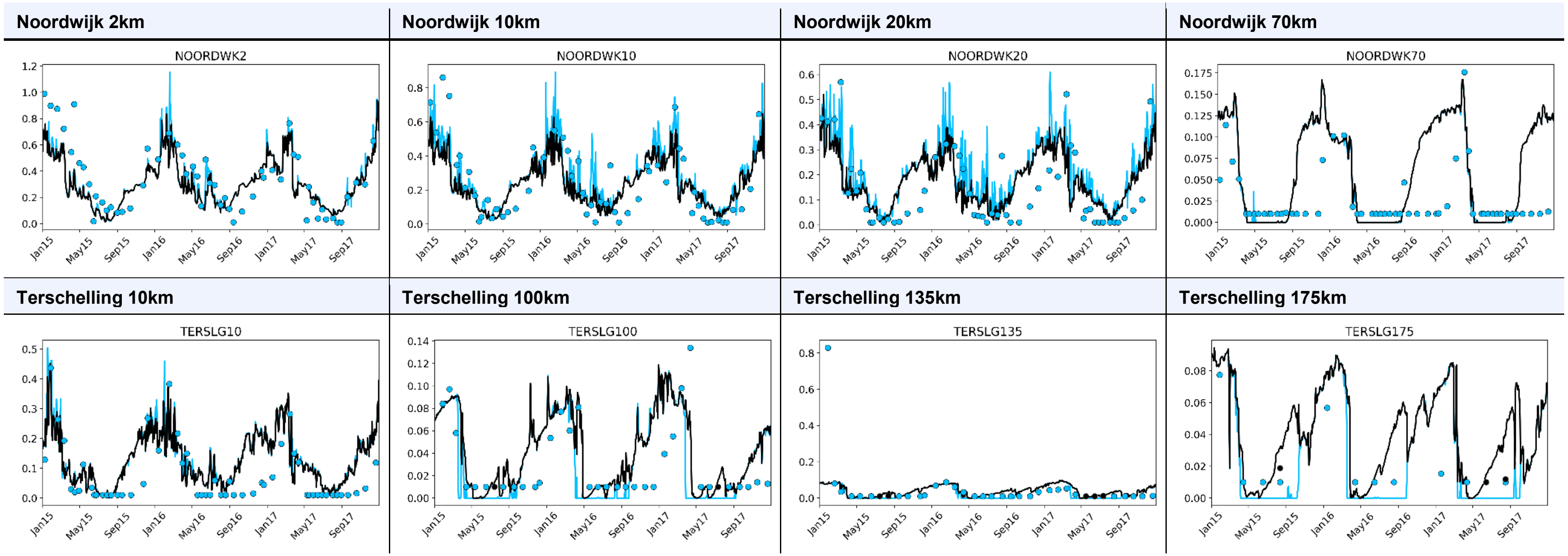

Figure 3-9: Comparison of simulated (lines) and observed (dots) of nitrate (in mgN/L) near the surface (blue) and near the bottom (black) concentration along the Noordwijk and Terschelling MWTL transect. Note that the y-axes vary per figure.

3.3.2 Phosphate

The spatial variability of simulated winter mean phosphate concentrations shows a good correspondence with in-situ observations in near-shore coastal waters and shelf areas around the North Sea and river plumes (Figure 3-10 and Figure 3-11). In the Kattegat area, phosphate concentrations are underestimated, particularly along the German and Danish coasts.

As shown in Table 3-4 and Figure 3-12, the model reproduces monthly-average near-surface phosphate concentrations better in near-shore and offshore waters, further than 100 km from the coast. At these locations the model performs very well in terms of correlations. Performance in terms of nRMSE is overall only satisfactory, probably due to the underestimation of phosphate concentrations during the growing season. Correlations are lower in areas at intermediate distances from the coast, such as NOORDWK 10-70 and TERSLG 10-100.

The seasonal variability in the 3D DCSM-FM model, compared to time series of in-situ observations shows that simulated concentrations are generally well in line with observations in winter, but too low in summer (Figure 3-13). In the model PO4 concentrations go down to zero, whereas in observations they are not consistently at the detection limit. This suggests that the model may overestimate phosphorus uptake by phytoplankton during the summer months, particularly near shore.

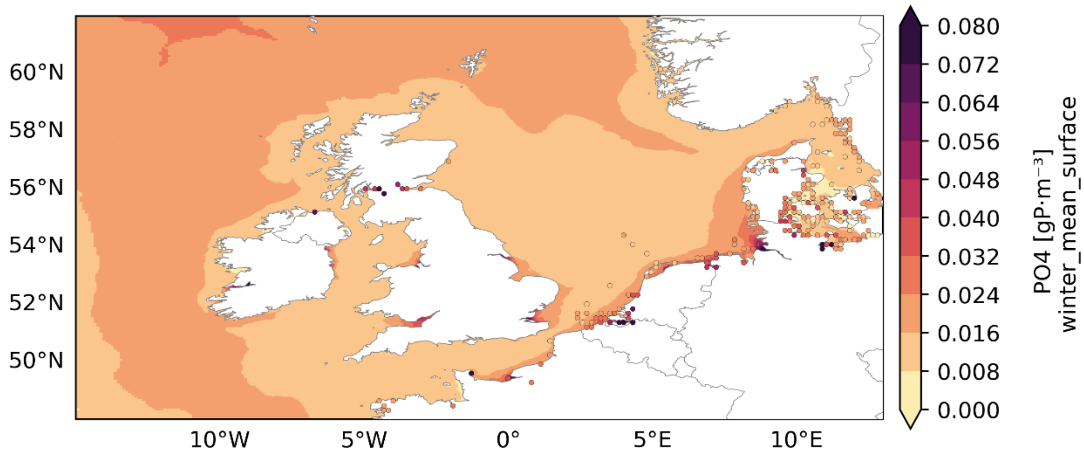

Figure 3-10: Simulated (background) and observed (dots) phosphate winter mean concentration near-surface for 2015-2017.

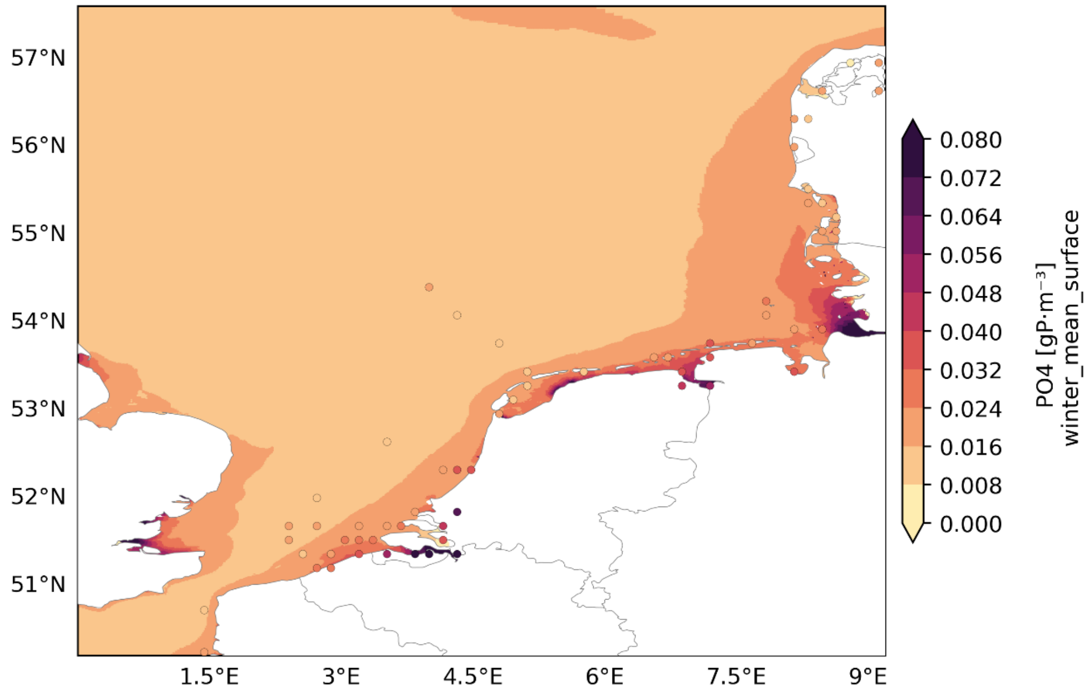

Figure 3-11:Simulated (background) and observed (dots) phosphate winter mean concentration near-surface for 2015-2017, zoomed into the Southern North Sea.

Table 3-4: Skill metrics for monthly-average near-surface phosphate concentrations at MWTL stations. Colours refer to the evaluation criteria categories from Table 3-1.

Station	Number of months	Mean Obs	Mean DCSM	Std Dev Obs	Std Dev DCSM	Correlation	RMSE	nRMSE
WALCRN2	12	0.018	0.011	0.007	0.01	0.868	0.008	1.14
WALCRN20	12	0.012	0.011	0.005	0.008	0.881	0.005	1.00
WALCRN70	12	0.008	0.009	0.004	0.006	0.767	0.004	1.00
NOORDWK2	12	0.022	0.011	0.009	0.01	0.901	0.012	1.33
NOORDWK10	12	0.017	0.01	0.009	0.009	0.625	0.011	1.22
NOORDWK20	12	0.012	0.009	0.006	0.008	0.562	0.008	1.33
NOORDWK70	12	0.01	0.007	0.005	0.006	0.254	0.007	1.40
TERSLG10	12	0.009	0.007	0.004	0.007	0.538	0.007	1.75
TERSLG100	12	0.014	0.006	0.009	0.005	0.541	0.011	1.22
TERSLG135	12	0.011	0.006	0.005	0.005	0.857	0.006	1.20
TERSLG175	4	0.008	0.004	0.003	0.005	0.865	0.005	1.67
TERSLG235	4	0.009	0.005	0.003	0.006	0.959	0.005	1.67
ROTTMPT3	12	0.014	0.011	0.005	0.011	0.551	0.01	2.00
ROTTMPT50	4	0.006	0.001	0.001	0.002	0.396	0.005	5.00
ROTTMPT70	4	0.006	0.001	0.001	0.002	0.087	0.005	5.00

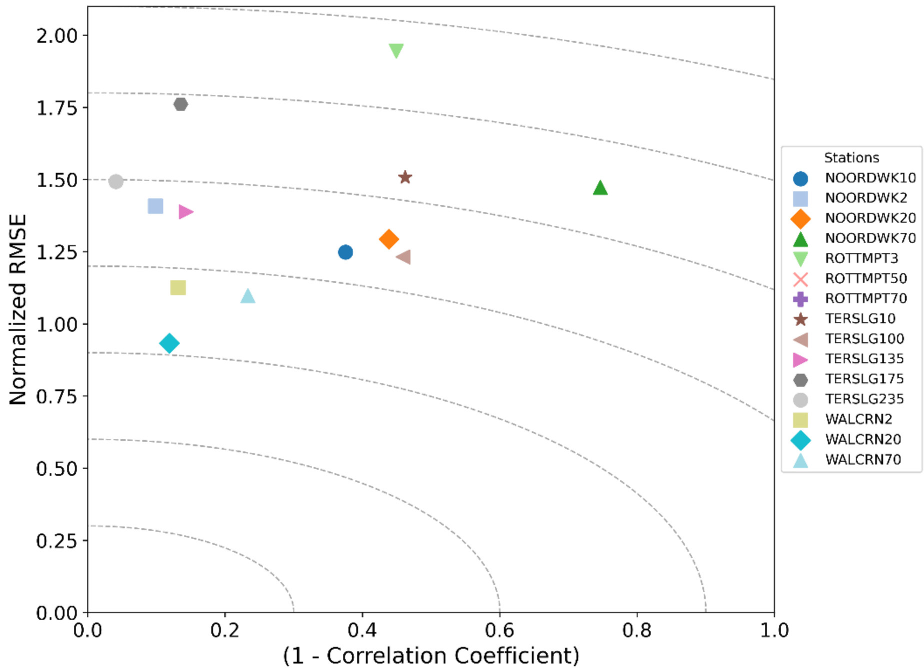

Figure 3-12: Model skill assessment for monthly-average near-surface phosphate at the MWTL stations over 2015-2017.

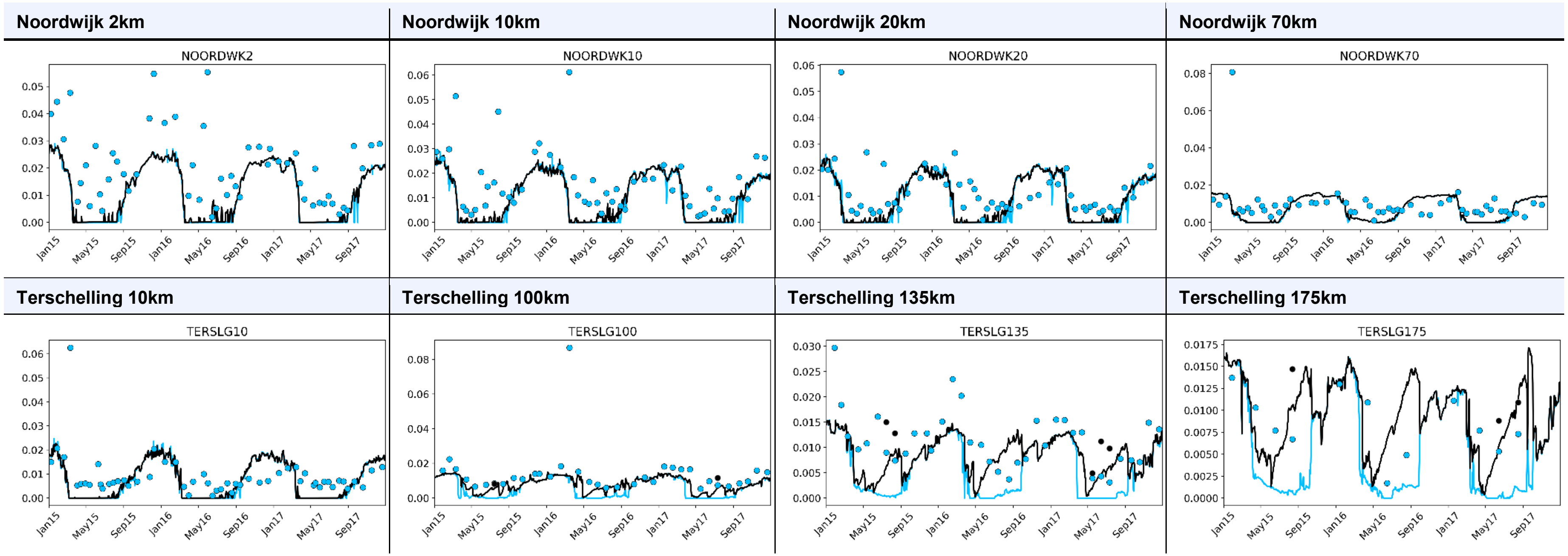

Figure 3-13: Comparison of simulated (lines) and observed (dots) of phosphate (in mgP/L) near the surface(blue) and near the bottom (black) concentration along the Noordwijk and Terschelling MWTL transect. Note that the y-axes vary per figure.

3.3.3 Chlorophyll-a

The spatial variability of simulated growing-season near-surface chlorophyll-a concentrations shows a good correspondence with in-situ observations, with higher concentrations along the Southern North Sea coast and in river plumes, and lower concentrations offshore (Figure 3-14 and Figure 3-15).

Comparison with satellite data (Figure 3-14 vs Figure 3-16) confirms that the 3D DCSM-FM model captures the observed spatial patterns, with elevated chlorophyll-a concentrations in the southern North Sea, Irish Sea, Scottish coastal waters and the Norwegian Trench. The model tends to underestimate growing-season near-surface chlorophyll-a in coastal waters compared to satellite data and overestimate offshore concentrations (Figure 3-17). Simulated concentrations are more strongly underestimated in the Baltic Sea. This is likely (partly) due to the underestimation of winter mean phosphate concentrations by the model in that region.

Comparing the variability of monthly-average chlorophyll-a concentrations simulated with 3D DCSM-FM model with satellite data aggregated per OSPAR eutrophication assessment area shows that it is best reproduced in the shelf waters of the Celtic and northern North Sea, with correlation coefficients close to 1 (Figure 3-18). Also in coastal waters of the southern and eastern North Sea and Norwegian Trench the seasonal variability is well reproduced with correlation coefficients close to 0.7. In river plumes, Scottish coastal waters and the Irish Sea the seasonal variability of chlorophyll-a is less well reproduced, with correlation coefficients below 0.4.

According to comparison with in-situ measurements (Table 3-5 and Figure 3-19), the model outputs shows some very good correlation with observations in coastal waters (e.g. 0,83 at WALCRN2, 0,73 at NOORDWK2). This is contradictory with the lower correlation coefficients found in river plumes when comparing with satellite data. This is due to the fact that the satellite product used for comparison here is less reliable in coastal, more turbid waters. The model skill metrics at MWTL stations also show that the model tends to underestimated chlorophyll-a variability near the coasts and over-estimating it at more offshore stations (e.g. along the Terschelling transect).

Comparison with time series of in-situ observations along the Noordwijk and Terschelling transects shows that the 3D DCSM-FM water quality model simulates clear spring blooms and often also an autumn bloom (Figure 3-20). In coastal waters (up to 20 km from shore) the magnitude and timing of these blooms largely corresponds with the in-situ and satellite observations. Offshore these blooms are often larger than the observed data. In winter simulated chlorophyll-a levels offshore are down to zero, which is lower than the observations. If using these model outputs for the simulation higher trophic levels, this may hamper the survival of modelled secondary producers (e.g. zooplankton populations) over winter. On the other hand, including zooplankton to the model might also improve simulated phytoplankton dynamics, leading to reduce growth in summer due to grazing and increased growth in winter due to changes in nutrient turnover.

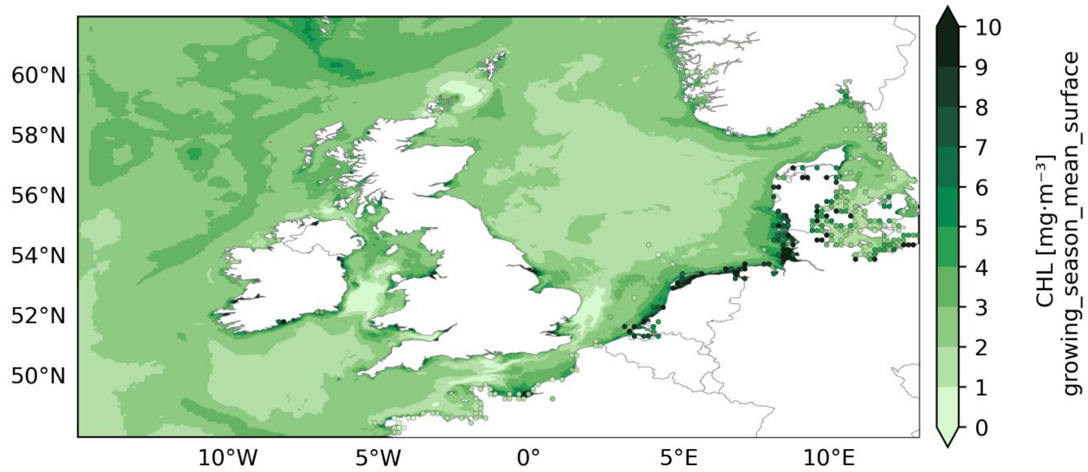

Figure 3-14: Simulated (background) and observed (dots) growing season mean near-surface chlorophyll-a concentration for 2015-2017.

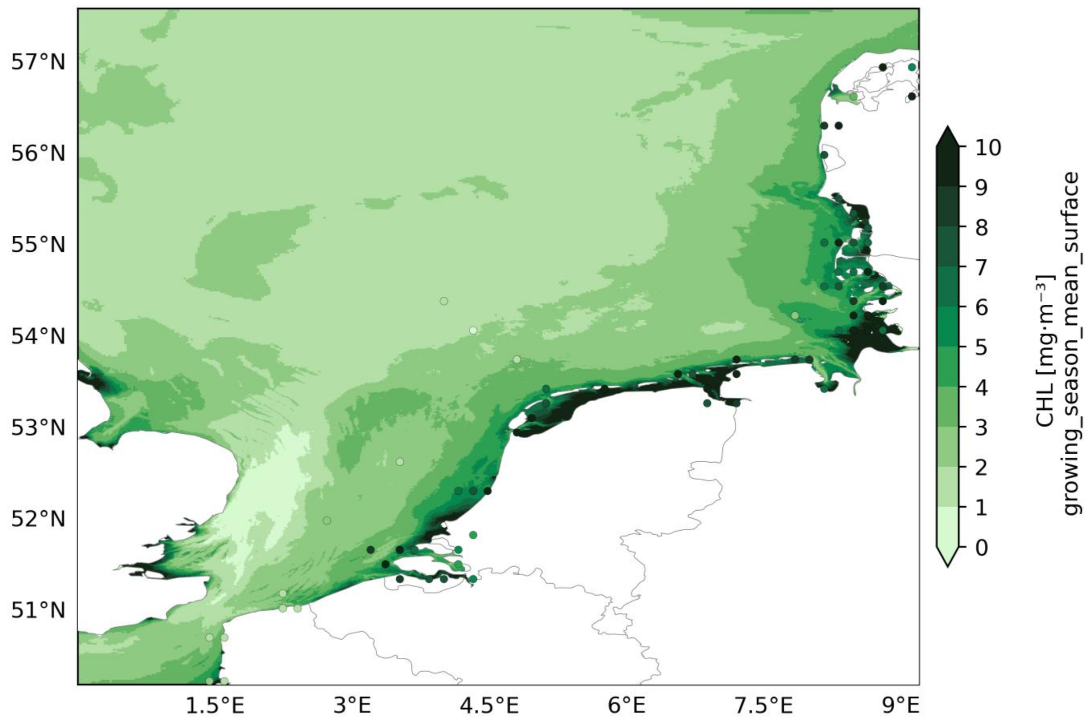

Figure 3-15: Simulated (background) and observed (dots) growing season mean near-surface chlorophyll-a concentration for 2015-2017, zoomed into the Southern North Sea.

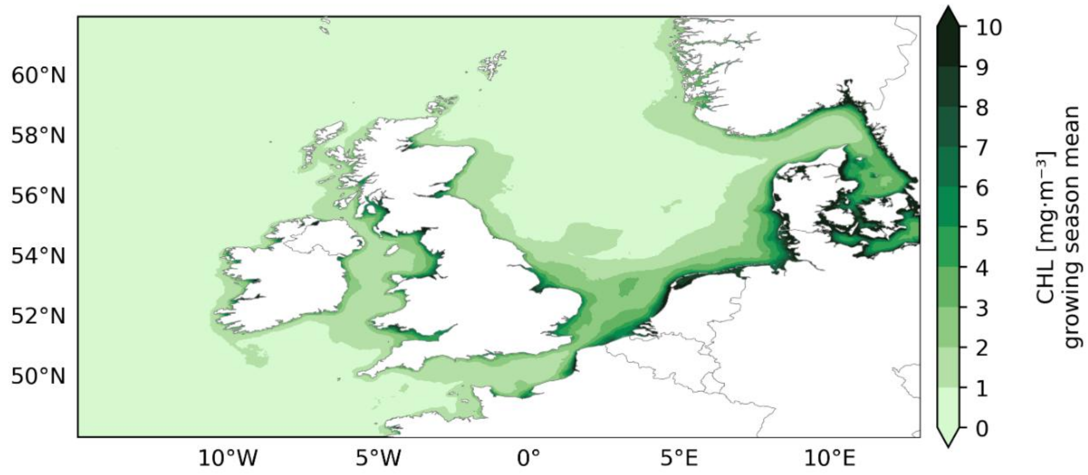

Figure 3-16: Sentinel 2 observed growing season mean near-surface chlorophyll-a concentration for 2015-2017.

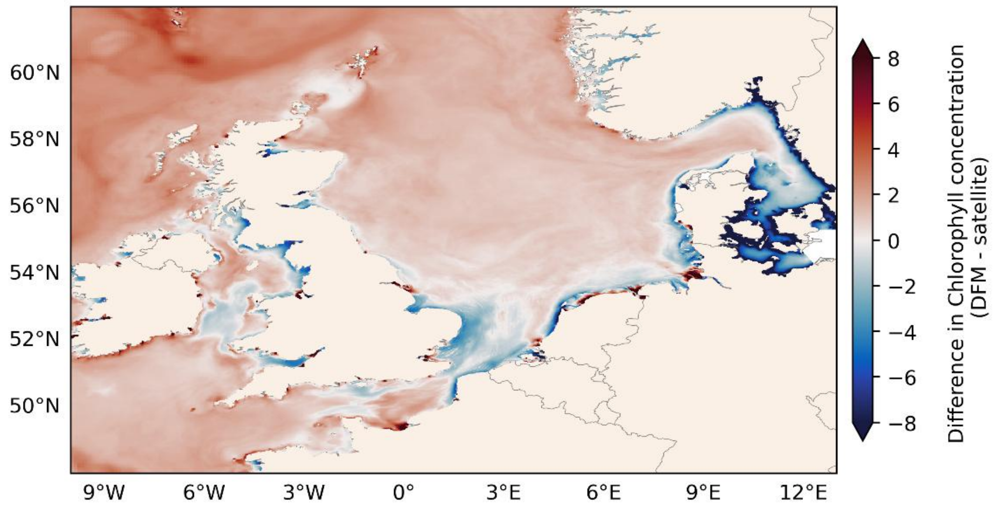

Figure 3-17: Absolute difference between simulated growing-season near-surface chlorophyll-a and satellite observations for 2015-2017.

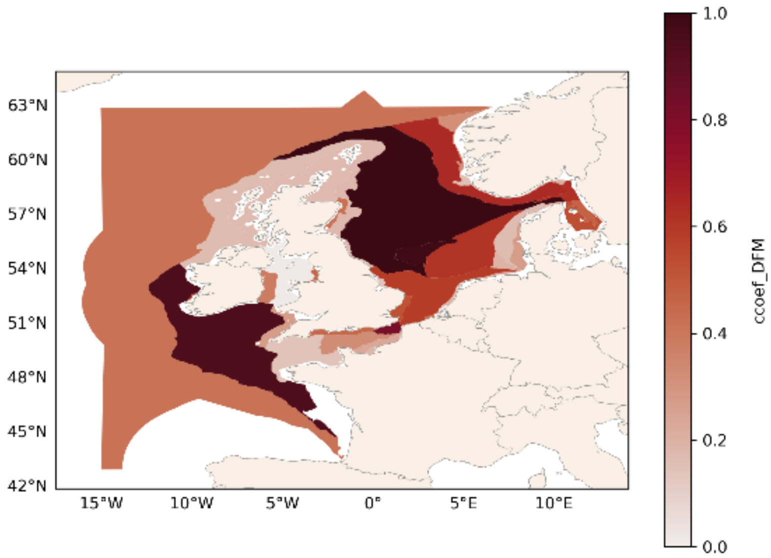

Figure 3-18: Correlation coefficient between simulated and satellite monthly-average near-surface chlorophyll-a concentrations over 2015-2017 growing seasons and aggregated per OSPAR assessment area.

Table 3-5: Skill metrics for monthly-average near-surface chlorophyll-a concentrations at MWTL stations, aggregated across all months and all three years (2015-2017) combined. Colours refer to the evaluation criteria categories from Table 3-1.

Station	Number of months	Mean Obs	Mean DCSM	Std Dev Obs	Std Dev DCSM	Correlation	RMSE	nRMSE
WALCRN2	12	9.76	2.76	9.73	2.37	0.83	10.54	1.08
WALCRN20	12	5.59	2.02	6.95	2.12	0.88	6.29	0.91
WALCRN70	12	2.09	1.41	2.86	2.17	0.31	3.09	1.08
NOORDWK2	12	6.99	3.63	5.71	2.73	0.73	5.34	0.94
NOORDWK10	12	5.34	3.6	3.74	2.68	0.66	3.32	0.89
NOORDWK20	12	4.84	3.37	2.53	2.73	0.78	2.28	0.90
NOORDWK70	12	1.42	1.38	0.62	1.68	0.51	1.47	2.37
TERSLG10	12	4.19	2.68	4.25	2.49	0.12	4.9	1.15
TERSLG100	12	0.86	1.11	0.41	1.51	0.75	1.26	3.07
TERSLG135	12	1.04	0.84	0.59	1.16	0.4	1.09	1.85
TERSLG175	4	0.58	0.88	0.25	0.95	0.94	0.78	3.12
TERSLG235	4	0.6	0.98	0.21	0.79	0.38	0.82	3.90
ROTTMPT3	12	7.52	3.54	5.87	2.4	0.54	6.4	1.09
ROTTMPT50	4	1.94	1.93	0.69	0.41	-0.87	1.06	1.54
ROTTMPT70	4	1.47	1.73	0.2	0.4	-1.0	0.65	3.25

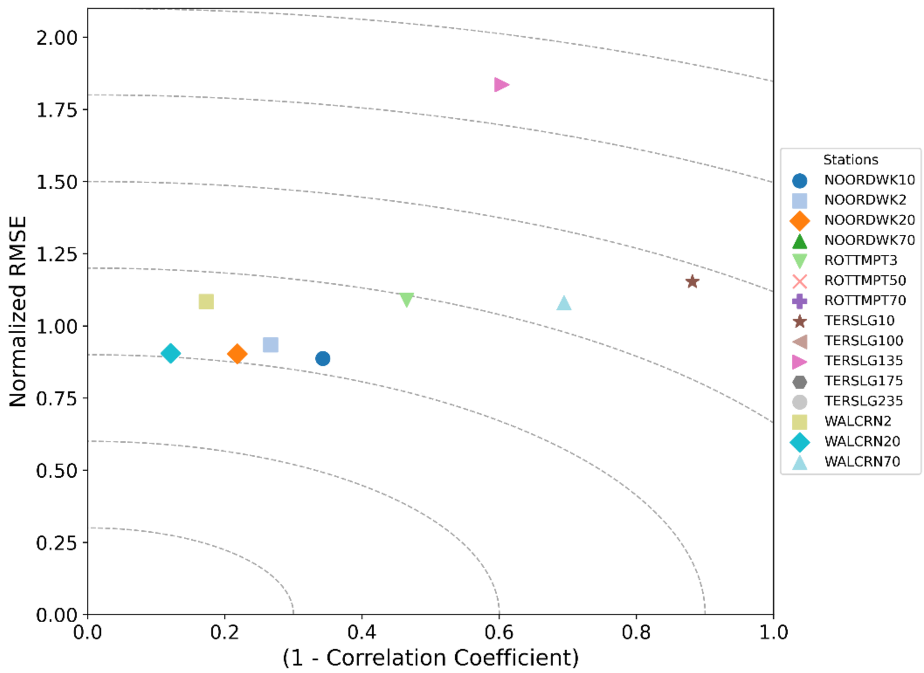

Figure 3-19: :Model skill assessment for monthly-average near-surface chlorophyll-at the MWTL stations over 2015-2017.

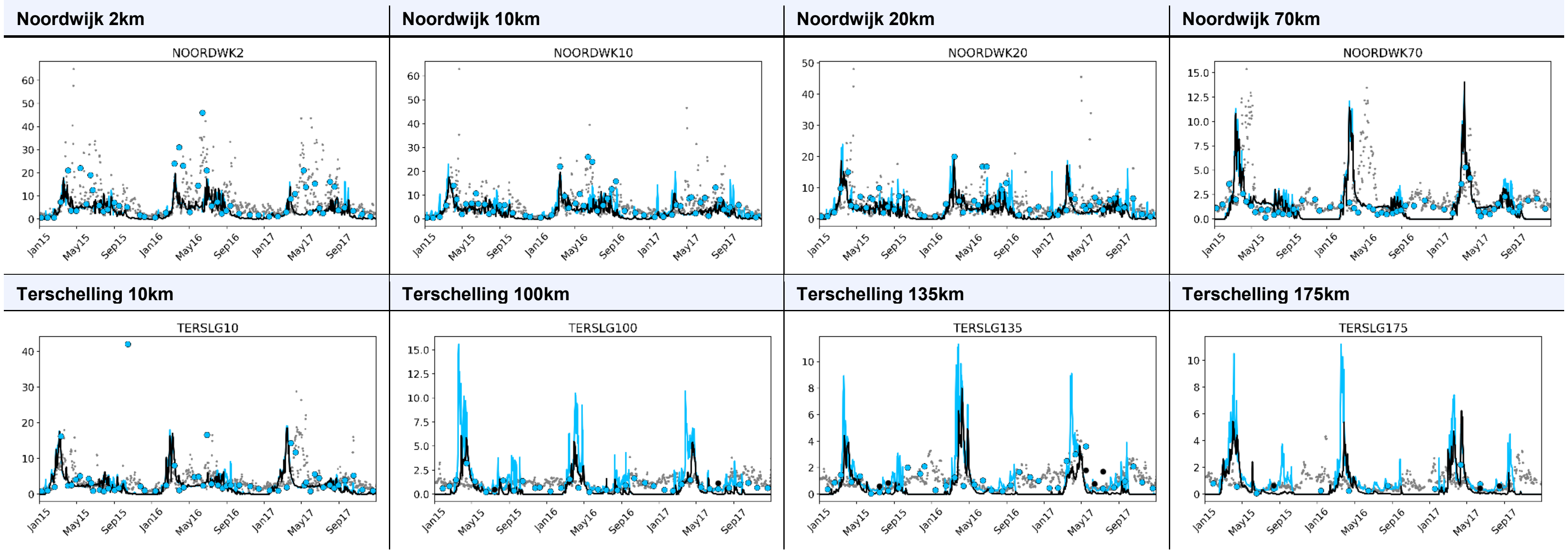

Figure 3-20: Comparison of simulated (lines) and observed (bigger dots) of chlorophyll-a (in µg/L) near the surface (blue) and near the bottom (black) along the Noordwijk and Terschelling MWTL stations. Grey, smaller dots are satellite data. Note that the y-axes vary per figure.

3.3.4 Dissolved oxygen

The 3D DCSM-FM model results for summer mean surface oxygen show a spatial pattern with lower concentrations in shallow coastal and shelf regions, and higher concentrations in deeper offshore areas (Figure 3-21 and Figure 3-22). In many areas of the model domain (particularly in east of Denmark and in Irish nearshore regions), simulated surface oxygen concentrations are generally higher than observed values. Discrepancies in the Baltic area might be linked to the underestimation of primary production in that area by the model, that could then lead to lower amounts of detrital organic matter produced in the system and subsequently lower oxygen demand for re-mineralization.

Model skill metrics for monthly-average near-surface dissolved oxygen indicate overall a good to very good performance in terms of correlation with measurements, with strongest correlations closest to the coast (Table 3-6 and Figure 3-23). Correlation between model and in-situ observations is >0.6 at all MWTL stations and mostly above 0.8. Both yearly means and variability of monthly average concentrations for the period 2015-2017 are well captured by the model. The model performs satisfactorily at most stations in terms of nRMSE. nRMSE values larger than 1 likely occur because of the overestimation of winter concentrations in the model.

Time series comparisons at selected monitoring stations reveal that the 3D DCSM-FM model captures the summer minima in oxygen concentrations reasonably well, but tends to overestimate concentrations during winter months (Figure 3-24). This overestimation is stronger at more offshore locations (e.g. TERSLG135 and 175), which might be due to an overestimation of re-oxygenation at the atmosphere-water interface and can be partly due to an overestimation of primary production at the end of the winter period (e.g. March).

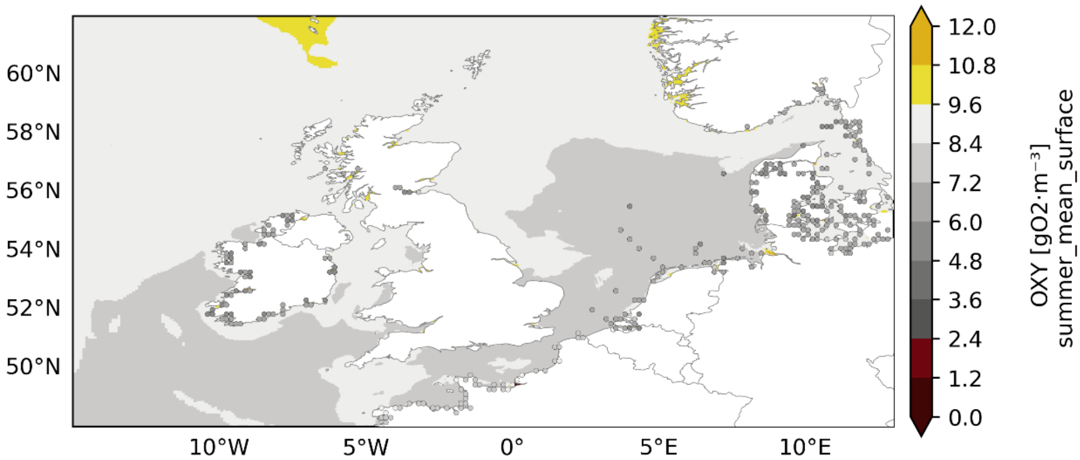

Figure 3-21: Simulated (background) and observed (dots) summer mean near-surface dissolved oxygen for 2015-2017.

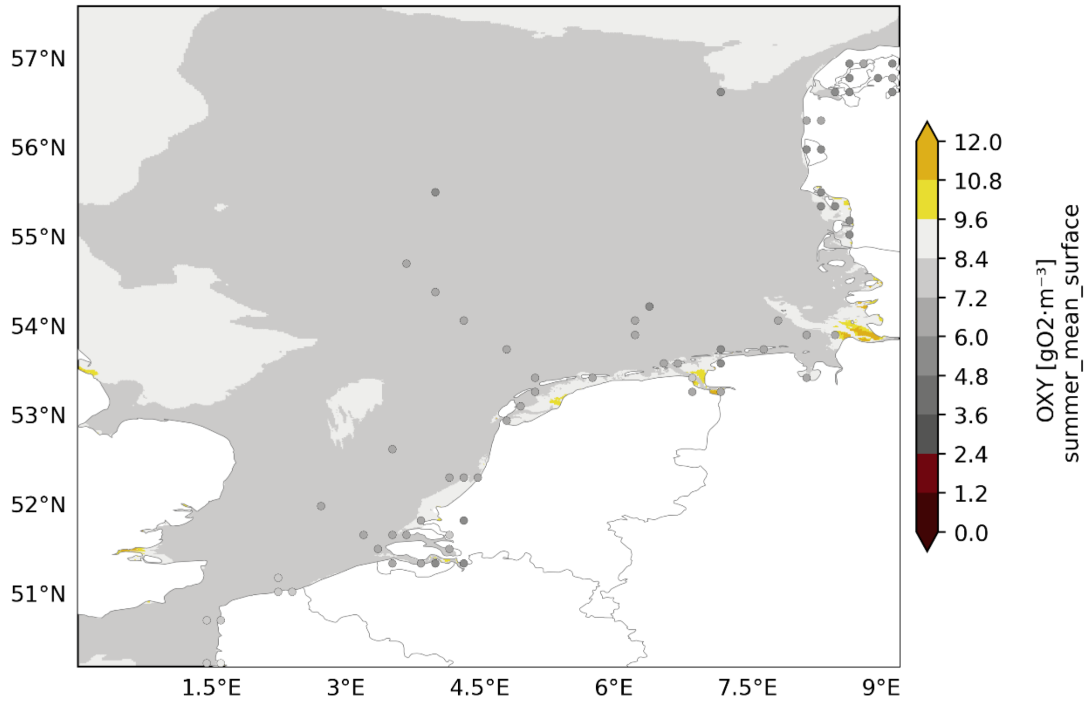

Figure 3-22: Simulated (background) and observed (dots) summer mean near-surface dissolved oxygen concentration for 2015-2017, zoomed into the Southern North Sea.

Table 3-6: Skill metrics for monthly-average near-surface dissolved oxygen concentrations at MWTL stations. Colours refer to the evaluation criteria categories from Table 3-1.

Station	Number of months	Mean Obs	Mean DCSM	Std Dev Obs	Std Dev DCSM	Correlation	RMSE	nRMSE
WALCRN2	12	8.25	9.0	0.91	1.02	0.82	0.96	1.05
WALCRN20	12	8.1	8.81	1.1	1.07	0.84	0.95	0.86
WALCRN70	12	7.9	8.67	0.77	0.91	0.93	0.85	1.10
NOORDWK2	12	8.23	9.2	0.9	1.1	0.77	1.2	1.33
NOORDWK10	12	8.4	9.17	0.6	1.09	0.85	1.02	1.70
NOORDWK20	12	8.28	9.09	0.68	1.07	0.64	1.16	1.71
NOORDWK70	12	7.77	8.76	0.71	0.93	0.61	1.25	1.76
TERSLG10	12	8.09	8.99	0.78	1.1	0.86	1.08	1.38
TERSLG100	12	8.21	8.95	0.65	0.95	0.85	0.91	1.40
TERSLG135	12	8.15	8.94	0.8	0.91	0.84	0.93	1.16
TERSLG175	4	8.19	9.04	0.5	0.89	0.9	0.98	1.96
TERSLG235	4	7.88	9.04	0.7	0.78	0.85	1.24	1.77
ROTTMPT3	12	9.04	9.31	1.0	1.19	0.97	0.44	0.44
ROTTMPT50	4	7.53	8.34	0.25	0.72	0.92	0.96	3.84
ROTTMPT70	4	7.59	8.37	0.42	0.71	0.92	0.87	2.07

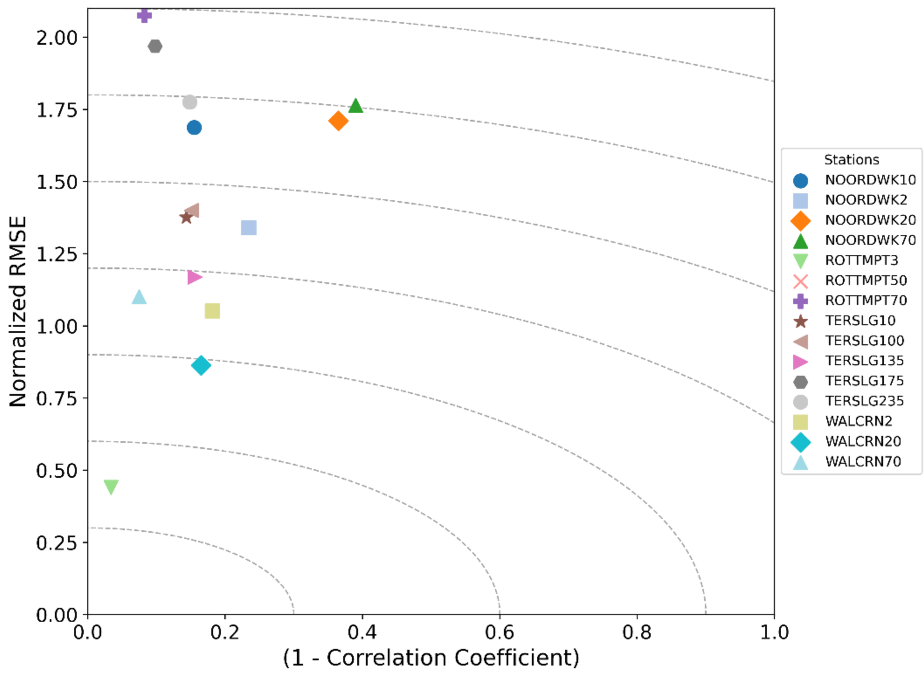

Figure 3-23: Model skill assessment for monthly-average near-surface dissolved oxygen at the MWTL stations over 2015-2017.

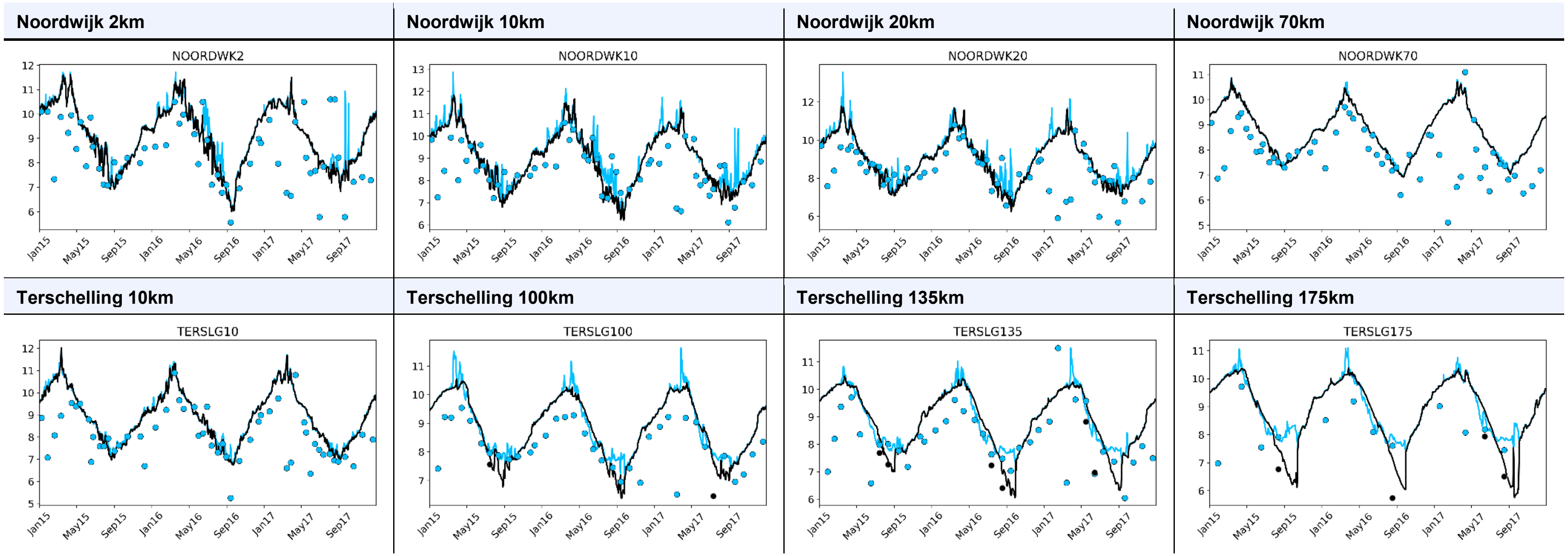

Figure 3-24: Comparison of simulated (line) and observed (dots) of dissolved oxygen (in mgO_2/L) near the surface and near the bottom along the Noordwijk and Terschelling MWTL transects. Note that the y-axes vary per figure.

4 Model applications, limitations and next steps

This model version has been validated by comparing with in-situ and remote sensing measurements for the 2015-2017 period and a previous version of it was compared with other models from OSPAR's ICG-EMO working group (Lenhart et al., 2022). The model setup was defined together with other ICG-EMO modelling institutes and model results have been used for policy applications within this context. This model set-up has also served as base in a number of research projects, for example with applications on large-scale upscaling of low trophic aquaculture in the North Sea (e.g. within the EDITO Model Lab project).

The present model-observation comparisons as well as previous reports show that this model performs very well for the simulation of temperature, stratification and winter nutrient concentrations. Results show that overall the model tends to underestimate phosphate in summer and overestimates nitrate, likely pointing to the fact that phosphorus uptake by phytoplankton is too high and nitrogen re-mineralization rates might be overestimated. Chlorophyll-a concentrations are overall well represented nearshore, but are systematically overestimated during the growing-season in offshore areas, which could also be partly caused by an overestimation of nitrogen re-mineralization rates in the summer. Simulated chlorophyll-a drops to zero in the winter at most stations, while low concentrations are measured in-situ. Winter dissolved oxygen seem to be slightly overestimated by the model, but summer minima are well captured.

Model validation has mostly focussed on the Dutch North Sea and comparison with MWTL data. However, map plots comparing the model outputs to international data from the NWDM database allow to have an idea about the model performance in other areas of the North Sea. Results show that the model for example should be improved to be used for interpretations in the Baltic Sea, where the model clearly underestimates phosphate and chlorophyll-a concentrations and overestimates dissolved oxygen, probably due to an underestimation of phosphorus at the Baltic inflow boundaries. It would be beneficial for future schematization releases to refine the validation in areas outside of the Dutch North Sea, for example by aggregating skill metrics results over OSPAR assessment areas. This would enhance confidence in the model's reliability across other regions of the North Sea and adjacent waters and improve its applicability for addressing transboundary issues (e.g. nutrient and pollutant transport, ecosystem impacts). We could also consider comparing model outputs with other satellite products, more reliable for turbid waters such as the OSPAR satellite product that is used for eutrophication assessments.

In the present report, we also focussed the validation on the most commonly used variables used to assess biogeochemical functioning of marine waters. Based on a recent Wozep report investigating methods to implement zooplankton in the 3D DCSM-FM water quality model (Troost et al., 2025), we also suggest for future schematization releases to validate intermediate variables to assess the performance of the model in representing specific underlying processes. Depending on available observation data, this could for example include looking at light extinction in the water column, phytoplankton species composition or primary production.

The potential applications that can be carried out with the present model are limited by the processes included in the model. In this model version, inorganic suspended sediments are not simulated. These are forced using average yearly measurements from satellite data, over which a sinusoidal function is applied to approximate seasonal patterns. This means this version of the model is not directly applicable for management questions relating to activities

that could lead to changes in sediment dynamics (e.g. sand mining, offshore wind developments). A work around would be to simulate changes in sediment dynamics with a separate model and implement the resulting suspended sediment fields as input to the model version described in this report.
The model also doesn't simulate zooplankton dynamics, which limits its use for applications linking to effects on higher trophic levels. We recommend to include zooplankton in future versions, as this might improve the representation of phytoplankton dynamics in the model and since it is a crucial link to understanding changes in transfers through the marine food chain.

5 References

Agatova, A. I., Lapina, N. M., & Torgunova, N. I. (2008). Organic matter of the North Atlantic. *Oceanology*, *48*(2), 182–195. https://doi.org/10.1134/S0001437008020045

Bentzon-Tilia, M., Traving, S. J., Mantikci, M., Knudsen-Leerbeck, H., Hansen, J. L. S., Markager, S., & Riemann, L. (2015). Significant N2 fixation by heterotrophs, photoheterotrophs and heterocystous cyanobacteria in two temperate estuaries. *The ISME Journal*, *9*(2), 273–285. https://doi.org/10.1038/ismej.2014.119

Blauw, A. N., Los, H. F. J., Bokhorst, M., & Erftemeijer, P. L. A. (2009). GEM: a generic ecological model for estuaries and coastal waters. *Hydrobiologia*, *618*(1), 175. https://doi.org/10.1007/s10750-008-9575-x

Brzezinski, M. A. (1985). THE Si:C:N RATIO OF MARINE DIATOMS: INTERSPECIFIC VARIABILITY AND THE EFFECT OF SOME ENVIRONMENTAL VARIABLES 1. *Journal of Phycology*, *21*(3), 347–357. https://doi.org/10.1111/j.0022-3646.1985.00347.x

Deltares. (2023a). *D-Flow Flexible Mesh. Technical Reference Manual*.

Deltares. (2023b). *D-Water Quality Processes Library Description*.

Kooijman, B. (2009). *Dynamic Energy Budget Theory for Metabolic Organisation*. Cambridge University Press. https://doi.org/10.1017/CBO9780511805400

Lenhart, H.-J., Blauw, A. N., Desmit, X., Fernand, L., Friedland, R., Heyden, B., Kerimoglu, O., Lacroix, G., van der Linden, A., van der Molen, J., Plus, M., Prins, T., Ruvalcaba Baroni, I., Silva, T., Stegert, C., Thewes, D., Troost, T. A., Vilmin, L., & van Leeuwen, S. (2022). *ICG-EMO report on model comparison for historical scenarios as basis to derive new threshold values. London, OSPAR, Publication Number: 895/2022, 66 pp.*

Letscher, R. T., Moore, J. K., Teng, Y.-C., & Primeau, F. (2015). Variable C : N : P stoichiometry of dissolved organic matter cycling in the Community Earth System Model. *Biogeosciences*, *12*(1), 209–221. https://doi.org/10.5194/bg-12-209-2015

Los, F. J., & Blaas, M. (2010). Complexity, accuracy and practical applicability of different biogeochemical model versions. *Journal of Marine Systems*, *81*(1–2), 44–74. https://doi.org/10.1016/j.jmarsys.2009.12.011

Los, F. J., & Brinkman, J. J. (1988). Phytoplankton modelling by means of optimization: A 10-year experience with BLOOM II. *SIL Proceedings, 1922-2010*, *23*(2), 790–795. https://doi.org/10.1080/03680770.1987.11899715

Lovato, T., Butenschön, M., Tjiputra, J., & Negrel, J. (2024). *Report on ESMs performance and ranking at regions of interest for downscaling purposes.* https://doi.org/10.5281/zenodo.10821517

Meybeck, M. (1982). Carbon, nitrogen, and phosphorus transport by world rivers. *American Journal of Science*, *282*(4), 401–450. https://doi.org/10.2475/ajs.282.4.401

Nechad, B., Ruddick, K. G., & Park, Y. (2010). Calibration and validation of a generic multisensor algorithm for mapping of total suspended matter in turbid waters. *Remote Sensing of Environment*, *114*(4), 854–866. https://doi.org/10.1016/j.rse.2009.11.022

Prins, T., Blauw, A., Vilmin, L., van der Heijden, L., Heye, S., & Buckman, L. (2023). *Modelling of nutrient load scenarios and transboundary nutrient transport. A model study for OSPAR regions II, III and IV. Report 11209731-000-ZKS-0003*.

Prins, T. C., Blauw, A. N., Vilmin, L., van der Linden, A., & Troost, T. A. (2021). *Coherent assessment framework for eutrophication. Model results Deltares. 11206044-000-ZKS-0002, Deltares, Delft*.

Redfield, A. C. (1934). On the proportions of organic derivatives in sea water and their relation to the composition of plankton. In *James Johnston Memorial Volume* (pp. 176–192). University Press of Liverpool.

Seitzinger, S. P., Harrison, J. A., Dumont, E., Beusen, A. H. W., & Bouwman, A. F. (2005). Sources and delivery of carbon, nitrogen, and phosphorus to the coastal zone: An overview of Global Nutrient Export from Watersheds (NEWS) models and their application. *Global Biogeochemical Cycles*, *19*(4). https://doi.org/10.1029/2005GB002606

Troost, T. A., Wijsman, J. W. M., Saraiva, S., & Freitas, V. (2010). Modelling shellfish growth with dynamic energy budget models: an application for cockles and mussels in the Oosterschelde (southwest Netherlands). *Philosophical Transactions of the Royal Society B: Biological Sciences*, *365*(1557), 3567–3577. https://doi.org/10.1098/rstb.2010.0074

Troost, T., Rienstra, J., Schneider, L., Vilmin, L., & Heye, S. (2025). *North Sea Trophic transfer modelling, Progress report. 11211547-002-ZKS-0001, Deltares, Delft (Preliminary version, submitted)*.

van der Kaaij, T., van Kessel, T., Troost, T., Herman, P., van Duren, L., & Villars, N. (2017). *Modelondersteuning MER winning suppletie- en ophoogzand Noordzee 2018 – 2027. Modelvalidatie. 1230888-002-ZKS-0006, Deltares, Delft*.

van Leeuwen, S. M., Lenhart, H.-J., Prins, T. C., Blauw, A., Desmit, X., Fernand, L., Friedland, R., Kerimoglu, O., Lacroix, G., van der Linden, A., Lefebvre, A., van der Molen, J., Plus, M., Ruvalcaba Baroni, I., Silva, T., Stegert, C., Troost, T. A., & Vilmin, L. (2023). Deriving pre-eutrophic conditions from an ensemble model approach for the North-West European seas. *Frontiers in Marine Science*, *10*. https://doi.org/10.3389/fmars.2023.1129951

Zijl, F., Laan, S. C., Emmanouil, A., van Zelst, V. T. M., van Kessel, T., Vilmin, L., & van Duren, L. A. (2021). *Potential ecosystem effects of large upscaling of offshore wind in the North Sea. Final report model scenarios. 11203731-004-ZKS-0015, Deltares, Delft*.

Zijl, F., Laan, S. C., & Groenenboom, J. (2021). *Development of a 3D model for the NW European Shelf (3D DCSM-FM). 11205259-015-ZKS-0003, Deltares, Delft*.

Zijl, F., Laan, S. C., Leumens, L., Zijlker, T., van Kessel, T., van Zelst, V. T. M., Jaksic, L., Vilmin, L., Schneider, L. K., & van Duren, L. A. (2023). *Scenario studies on potential ecosystem effects in future offshore wind farms in the North Sea. 11208071-001-ZKS-0010, Deltares, Delft*.

Zijl, F., Zijlker, T., Laan, S., & Groenenboom, J. (2023). *3D DCSM-FM: a sixth-generation model for the NW European Shelf (2022 release). Deltares, report 11208054-004-ZKS-0003, Delft*.

Deltares is an independent institute for applied research in the field of water and subsurface. Throughout the world, we work on smart solutions for people, environment and society.

Deltares

www.deltares.nl